Original Article
A novel combination therapy of arginine deiminase and an arginase inhibitor targeting arginine metabolism in the tumor and immune microenvironment

Pei-Hsuan Ye[1*], Chung-Yen Li[2*], Hao-Yu Cheng[3], Gangga Anuraga[4,5], Chih-Yang Wang[4], Feng-Wei Chen[2], Shiang-Jie Yang[2], Kuo-Ting Lee[6], Kwang-Yu Chang[7,8], Ming-Derg Lai[1,2]

[1]Department of Biochemistry and Molecular Biology, College of Medicine, National Cheng Kung University, Tainan, Taiwan, ROC; [2]Institute of Basic Medical Sciences, College of Medicine, National Cheng Kung University, Tainan, Taiwan, ROC; [3]Department of Biotechnology and Bioindustry Sciences, National Cheng Kung University, Tainan, Taiwan, ROC; [4]PhD Program for Cancer Molecular Biology and Drug Discovery, College of Medical Science and Technology, Taipei Medical University and Academia Sinica, Taipei, Taiwan, ROC; [5]Department of Biological Science, Faculty of Science and Technology, Universitas PGRI Adi Buana, Surabaya 60234, Indonesia; [6]Department of Surgery, National Cheng Kung University Hospital, College of Medicine, National Cheng Kung University, Tainan, Taiwan, ROC; [7]National Institute of Cancer Research, National Health Research Institutes, Tainan, Taiwan, ROC; [8]Department of Oncology, National Cheng Kung University Hospital, College of Medicine, National Cheng Kung University, Tainan, Taiwan, ROC. *Equal contributors.

Abstract: Tumor progression is dependent on tumor cells and their microenvironment. It is important to identify therapies that inhibit cancer cells and activate immune cells. Arginine modulation plays a dual role in cancer therapy. Arginase inhibition induced an anti-tumor effect via T-cell activation through an increase in arginine in the tumor environment. In contrast, arginine depletion by arginine deiminase pegylated with 20,000-molecular-weight polyethylene glycol (ADI-PEG 20) induced an anti-tumor response in argininosuccinate synthase 1 (ASS1)-deficient tumor cells. ADI-PEG 20 did not cause toxicity to normal immune cells, which can recycle the ADI-degraded product citrulline back to arginine. To target tumor cells and their neighboring immune cells, we hypothesized that the combination of an arginase inhibitor (L-Norvaline) and ADI-PEG 20 may trigger a stronger anticancer response. In this study, we found that L-Norvaline inhibits tumor growth in vivo. Pathway analysis based on RNA-seq data indicated that the differentially expressed genes (DEGs) were significantly enriched in some immune-related pathways. Significantly, L-Norvaline did not inhibit tumor growth in immunodeficient mice. In addition, combination treatment with L-Norvaline and ADI-PEG 20 induced a more robust anti-tumor response against B16F10 melanoma. Furthermore, single-cell RNA-seq data demonstrated that the combination therapy increased tumor-infiltrating CD8^{+} T cells and CCR7^{+} dendritic cells. The increase in infiltrated dendritic cells may enhance the anti-tumor response of CD8^{+} cytotoxic T cells, indicating a potential mechanism for the observed anti-tumor effect of the combination treatment. In addition, populations of immunosuppressive-like immune cells, such as *S100a8[+] S100a9[+]* monocytes and *Retnla[+] Retnlg[+]* TAMs, in tumors were dramatically decreased. Importantly, mechanistic analysis indicated that the processes of the cell cycle, ribonucleoprotein complex biogenesis, and ribosome biogenesis were upregulated after combination treatment. This study implied the possibility of L-Norvaline as a modulator of the immune response in cancer and provided a new potential therapy combined with ADI-PEG 20.

Keywords: ADI-PEG 20, arginase inhibitor, arginine metabolism, immune modulation, tumor microenvironment, single-cell RNA sequencing

Introduction

The last two decades have seen a growing interest in immunotherapies that exert a therapeutic response by regulating immune function, especially cancer treatment. The advantages of cancer immunotherapies are that they use the immune system to accomplish a highly specific, efficient, and continuous treatment for tumors. Recently, T-cell regulation has been an important index to predict the responses of cancer immunotherapy patients, especially

immune checkpoint therapy (anti-PD-1/PD-L1 or anti-CTLA-4 antibodies) [1]. Immune checkpoint therapy mainly blocks inhibitory receptors and maintains T-cell cytotoxicity. However, approximately 60-80% of patients with melanoma fail to respond to immunotherapy [2], indicating that there are different immunoregulatory mechanisms [3]. The alteration of T-cell metabolism or the activation process is an essential factor in T-cell activation and therapy response in cancer. For example, our previous study showed that skin delivery of indoleamine 2,3-dioxygenase (IDO; an enzyme that degrades tryptophan) siRNA induced an anti-tumor effect through cytotoxic T-cell activation [4]. In addition to tryptophan metabolism, arginine also regulates T-cell function. Arginase is an enzyme that transfers arginine into ornithine and urea and has two isoenzymes in humans, arginase 1 (ARG1) and arginase 2 (ARG2). Importantly, arginase expression is common in many immunosuppressive cells and mainly inhibits the effects of immunotherapy [5, 6]. Additionally, high expression of ARG2 in cancer cells was correlated with poor prognoses in patients with breast cancer [7]. Many arginases present in the tumor microenvironment (TME) may lead to arginine deficiency and T-cell dysfunction [8]. Moreover, exhaustion of extracellular arginine interferes with T-cell function through a decrease in CD3ζ expression, which is important for T-cell receptor (TCR) assembly and signal transduction [9, 10]. Furthermore, a lack of arginine induces G0/G1 phase cell cycle arrest in T cells via activation of the general control nondepressible 2 kinase-eukaryotic translation initiation factor axis (GCN2-eIF2α axis), leading to inhibition of protein synthesis and de novo DNA synthesis [11, 12]. Certain studies have indicated that ARG1-mediated arginine availability has an immunosuppressive role [13, 14]. Moreover, there is evidence that ARG2 can harm the anti-tumor immune response. ARG2 not only enhances Treg suppressive capacity but also inhibits the function and anti-tumor efficacy of DCs and CD8+ T cells [15-17].

Recently, it has been reported that arginase activity is elevated and considered a poor prognostic factor in various cancer types, including lung, colorectal, breast, ovarian and skin cancers [18-22]. In epithelial ovarian cancer, tumor cells release arginase-containing exosomes to alleviate the anti-tumor immune response [23].

Therefore, targeting arginase can be a therapeutic strategy for cancer treatment. Several arginase inhibitors have been developed [24], and their anti-tumor effects on different cancer types have been reported, such as N-hydroxy-nor-L-arginine (nor-NOHA) and Compound 9 (Cpd9) in lung cancer [25, 26]. However, most of them are competitive inhibitors and analogs of arginine. L-Norvaline is a potent noncompetitive arginase inhibitor [27]. Treatment with L-Norvaline alters the proportions of immune cells, such as regulatory T cells and type 17 helper T cells, in pulmonary fibrosis [28]. Alteration of NO by L-Novaline conferred antihyperglycemic effects in animal models [29, 30]. In addition, L-Norvaline may be a prospective neuroprotective molecule and has great potential for the treatment of neurodegenerative diseases such as Alzheimer's disease [27, 30-32]. However, the role of L-Norvaline in cancer treatment is not yet completely understood.

In argininosuccinate synthase 1 (ASS1)- and argininosuccinate lyase (ASL)-deficient tumor cells, exogenous arginine is mandatory for disease progression [33]. ASS1 and ASL are main enzymes to generate arginine from citrulline. Therefore, deprivation of arginine with arginine deiminase (ADI), a microbial enzyme that catalyzes arginine to citrulline and ammonia, can induce growth inhibitory in ASS1-deficient melanoma cell lines [34]. The pegylated form arginine deiminase (ADI-PEG 20) modified with polyethylene glycol extends the *in vivo* circulating half-life and immunogenicity reduction [35]. Clinical studies have shown ADI-PEG 20 to cause tumor responses in ASS-negative cancers and to decrease arginine rapidly but increase citrulline in serum concentration [36]. Recent studies have further suggested additive effect of ADI-PEG 20 with other anti-tumor agents, possibly extending its usage in ASS1-positive tumor [37, 38].

As noted above, immunotherapy efficacy is obviously obstructed by elevated levels of arginase produced by immunosuppressive cells in the TME. However, although some arginase inhibitors significantly inhibit tumor progression, whether L-Norvaline, a noncompetitive inhibitor, has anticancer therapeutic effects has been far less investigated. Given that arginine deprivation by ADI-PEG 20 rarely affect the production of immune cells [39], and that it
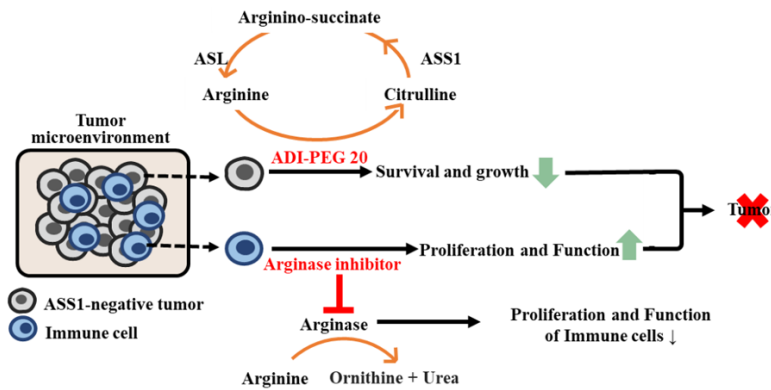
Figure 1. Hypothesis for the combination of L-Norvaline (arginase inhibitor) and ADI-PEG 20 anticancer potential. ADI-PEG 20 (an arginine-depleting agent) degrades arginine into citrulline, which can be recycled back into arginine in normal cells. However, ASS1-deficient tumor cells are sensitive to ADI-PEG 20 treatment since tumor cells lack the ASS1 enzyme to resynthesize arginine from citrulline. Moreover, arginase produced by some immunosuppressive cells or tumor cells degrades arginine and impairs the proliferation and function of immune cells in the tumor environment. Therefore, inhibition of arginase is expected to enhance tumor immunity. Based on decreased tumor growth and improved immune cell functions, the combination of L-Norvaline and ADI-PEG 20 is a potential therapeutic for cancer.

potentially result in increased T cells infiltration in TME [40, 41]. Therefore, we hypothesized combination with L-Norvaline to trigger stronger anticancer immune response in ASS1-negative tumor cells (**Figure 1**). To investigate the effects of combination treatment with ADI-PEG 20 and L-Norvaline, we observed tumor progression and immune cell alterations in tumor-bearing mouse models. Additionally, single-cell RNA sequencing was used to analyze the alteration of mechanisms and novel population findings in tumor-infiltrating immune cells.

This study demonstrates that L-Norvaline treatment could only inhibit tumor growth and regulate immune-related pathways in tumor cells. Additionally, the L-Norvaline-mediated anti-tumor effect was dependent on the immune system. ADI-PEG 20 treatment significantly enhanced the therapeutic effect on tumor regression induced by L-Norvaline or cisplatin. Moreover, combination treatment with L-Norvaline and ADI-PEG 20 increased infiltrated cytotoxic T cells and induced T-cell proliferation and riboprotein biogenesis. Interestingly, combination treatment also significantly decreased two populations of immunosuppressive-like immune cells, *S100a8*+ *S100a9*+ monocytes and *Retnla*+ *Retnlg*+ macrophages.

Results

L-Norvaline inhibits tumor progression via the immune system

Due to the multiple effects of arginine in tumor progression and activation of the immune system, we investigated the impact of L-Norvaline on immunocompetent mice. C57BL/6 mice were subcutaneously inoculated with both B16F10 melanoma cells and LL2 cells, and tumor development was monitored over time. When tumors were palpable, mice were treated with PBS or L-Norvaline. The treatment schedules for the two mouse models are described in **Figure 2A**. Treatment with 20 mg/kg or 100 mg/kg L-Norvaline did not cause weight loss in LL2 and B16F10 tumor-bearing mice (**Figure 2B** and Supplementary Figure 1A). In an orthotopic B16F10 melanoma mouse model, administration of 20 mg/kg L-Norvaline significantly suppressed tumor growth (**Figure 2C**). However, 20 mg/kg L-Norvaline showed no inhibitory effect on LL2 tumors; interestingly, a higher concentration (100 mg/kg) of L-Norvaline could slightly inhibit the growth of LL2 tumors (Supplementary Figure 1B). Due to the impact of arginine on the immune system and T cells activation, we hypothesized that the L-Norvaline-mediated anti-tumor response was dependent on immune system. We observed the tumor growth of B16F10 tumor-bearing immunodeficient mice (NOD-SCID mice) that received L-Norvaline. The results revealed that L-Norvaline had no therapeutic effect in tumor-bearing NOD-SCID mice (**Figure 2D**). These results indicate that L-Norvaline significantly restrained tumor growth in B16F10 tumor-bearing mice in a manner dependent on the immune system and did not cause toxic effects in mice.

L-Norvaline treatment is involved in immune-related pathways

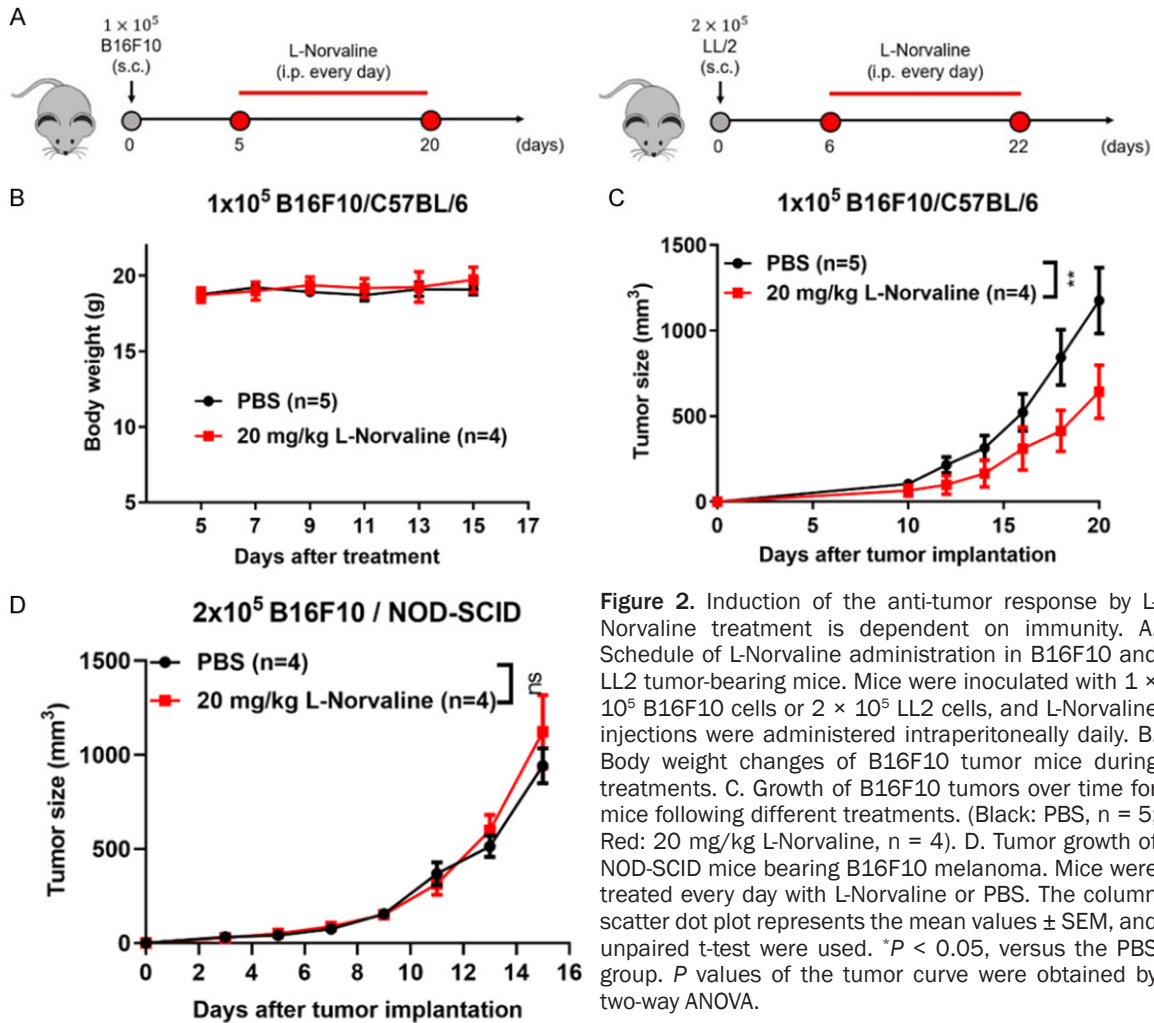Our data revealed that L-Norvaline inhibited tumor growth in the B16F10 mouse model. We

Figure 2. Induction of the anti-tumor response by L-Norvaline treatment is dependent on immunity. A. Schedule of L-Norvaline administration in B16F10 and LL2 tumor-bearing mice. Mice were inoculated with 1×10^5 B16F10 cells or 2×10^5 LL2 cells, and L-Norvaline injections were administered intraperitoneally daily. B. Body weight changes of B16F10 tumor mice during treatments. C. Growth of B16F10 tumors over time for mice following different treatments. (Black: PBS, n = 5; Red: 20 mg/kg L-Norvaline, n = 4). D. Tumor growth of NOD-SCID mice bearing B16F10 melanoma. Mice were treated every day with L-Norvaline or PBS. The column scatter dot plot represents the mean values ± SEM, and unpaired t-test were used. $^*P < 0.05$, versus the PBS group. P values of the tumor curve were obtained by two-way ANOVA.

first to identify whether L-Norvaline could regulate immunity, such as immune-related cytokines and inflammatory pathways, through tumor cells, we performed RNA sequencing of B16F10 cells treated with or without 0.1 mg/mL L-Norvaline and analyzed the enriched pathways of differentially expressed genes (DEGs) by the Metacore platform. We intersected genes with fold changes greater than or equal to 1.5 in the two experiments (**Figure 3A**). The pathway enrichment analysis with DEGs compared to the control group demonstrated that B16F10 cells treated with L-Norvaline were associated with immune reactions such as inflammation and cytokine production, neuron generation and other cellular processes. The "NETosis in SLE" and "Bone metastases in Prostate Cancer" were the most significant pathways in up- and down-regulated genes, respectively (**Figure 3B** and **3C**). To further

investigate these results, we carried out RNA-seq in B16F10 and LL2 cancer cell lines treated with or without 0.1 mg/mL L-Norvaline and incubated for 3 days (Supplementary Figure 2A). By dissecting the RNA-seq expression data between two cancer cells, 168 and 33 overlaps of upregulated (fold change ≥ 1.5) and down-regulated (fold change ≤ 1.5) genes, respectively, were identified (Supplementary Tables 1 and 2). To gain further insights into the functions of these DEGs, we used the online software Database for Annotation, Visualization and Integrated Discovery (DAVID) for KEGG pathway analyses. Both upregulated and down-regulated DEGs were significantly enriched in cytokine-cytokine receptor interactions (**Figure 3D**). In addition, MetaCore pathway analysis revealed that upregulated genes were involved in various immune-related pathways, such as the "immune response_IL-33 signaling path-
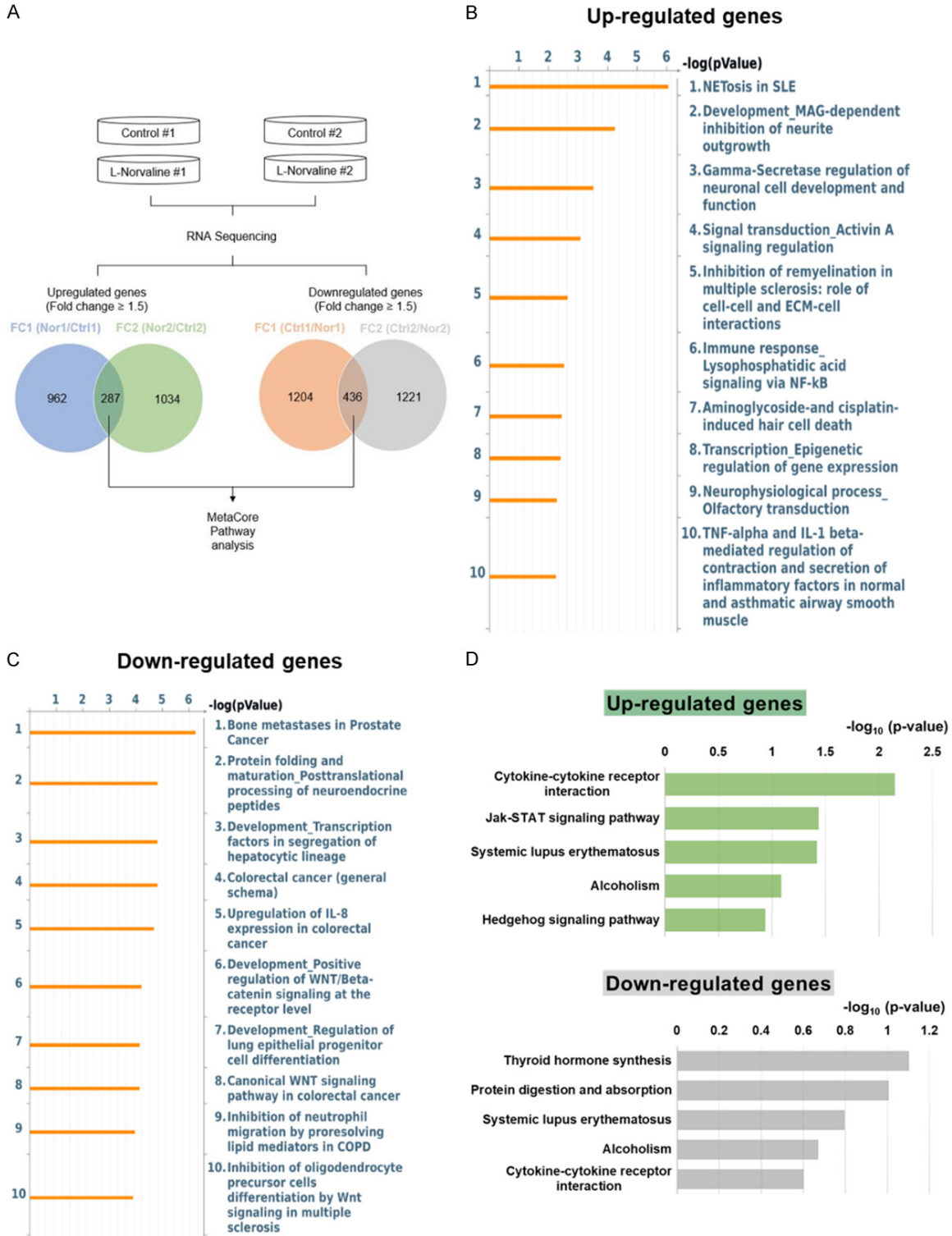
Figure 3. L-Norvaline treatment is involved in immune-related pathways. A. Flow chart of gene analysis. B16F10 cells were treated with or without 0.1 mg/mL L-Norvaline. RNA sequencing was performed in two independent experiments. Upregulated and downregulated genes with fold changes greater than or equal to 1.5 from the two experiments were selected and intersected. B. Bar chart showing the top 10 pathways enriched for 287 upregulated genes. C. Bar chart showing the top 10 pathways enriched for 436 downregulated genes. D. KEGG pathway enrichment analysis of differentially expressed genes in B16F10 and LL2 tumor cells treated with L-Norvaline by using the DAVID functional annotation tool. Bar chart showing the top 5 enriched pathways of upregulated and downregulated genes.

way", "immune response reactive oxygen species (ROS) in IL-4 signaling" and "eosinophil survival in asthma" (Supplementary Figure 2B). Taken together, by performing a bioinformatics analysis of DEGs, several immune-related pathways may be associated with the anticancer responses triggered by L-Norvaline. These findings showed that the anti-tumor effect of L-Norvaline might be induced by tumor cells by regulating immune-related genes.

Combination treatment of L-Norvaline with ADI-PEG 20 or an FDA-approved drug induces an additive effect on tumor inhibition

Previous results showed that L-Norvaline triggered anticancer responses with the aid of immunity. However, a lot of arginine in the TME provided the survival possibility of ASS1-deficient tumors. Thus, we were curious whether the combination of L-Norvaline and ADI-PEG 20 could induce additive tumor growth inhibition. We used the B16F10 melanoma mouse model to evaluate the impact of combining L-Norvaline and ADI-PEG 20 treatment on tumor growth since previous studies have reported that B16F10 tumors are arginine auxotrophic cancers. After 7 days of tumor implantation, L-Norvaline (20 mg/kg), ADI-PEG 20 (2 IU), or their combination was injected intraperitoneally (**Figure 4A**). Importantly, the combined treatment showed greater inhibitions of tumor volume and weight than L-Norvaline or ADI-PEG 20 alone (**Figure 4B** and **4C**). Next, to dissect the changes among tumor-infiltrating immune cell subsets following treatment with combination therapy, we applied flow cytometry. The numbers of CD4$^+$ and CD8$^+$ T cells were elevated (**Figure 4D** and **4E**). Together, these results suggest that the combination treatment was superior to the single agent in B16F10 melanoma tumors.

Conventional cancer therapeutics have been shown to regulate immune responses involved in therapeutic efficacy [42]. It has been reported that cisplatin not only causes DNA damage but also reduces the levels of immunosuppressive cells [43]. Therefore, we assumed that cisplatin might enhance the effect of L-Norvaline. To test this hypothesis, cisplatin and L-Norvaline were administered to B16F10 tumor-bearing mice, as illustrated in **Figure 4F**. L-Norvaline treatment in combination with cisplatin significi-

cantly reduced tumor size and weight compared with single treatment (**Figure 4G** and **4H**), indicating that combination treatment with L-Norvaline and cisplatin improved the antitumor response. Overall, these results suggest that the combination treatment of L-Norvaline with chemotherapy or arginine depletion is superior to the single agent in B16F10 melanoma tumors.

Combination treatment with L-Norvaline and ADI-PEG 20 causes an alteration of immune cells in the TME

To further investigate the signaling change in immune cells in the TME, we used single-cell RNA sequencing on a microwell-based system (BD Rhapsody) to evaluate this profile. Live tumor-infiltrating immune cells (CD45$^+$ and 7-AAD$^-$) were isolated from the L-Norvaline treatment, ADI-PEG 20 treatment, combination treatment and control groups. Then, we performed staining of CD45$^+$ cells with a BD sample tag, which carries a specific sequence, to identify the different groups during sequencing. After library construction and sequencing (the processes have been written in the Methods), we obtained 7334 cell information samples and further analyzed the gene information with the "Seurat" package.

First, we separated the cells into 15 clusters (Supplementary Figure 3A). Then, to identify different types of immune cells in each cluster, we analyzed the expression levels of common marker genes (*Cd3e* for T cells, *Cd14* for monocytes, *Adgre1* for macrophages, *H2-Aa* for dendritic cells (DCs), *Cd19* for B cells, and *Col1a1* for fibroblasts). The macrophage marker *Adgre1* (F4/80) was highly expressed in Clusters 0, 1, 8, 10, and 11 but not in Clusters 2 and 3; however, Clusters 2 and 3 had higher expression of *Cd14*. Additionally, Clusters 4, 6, 7, and 13 had a specific expression of *Cd3e* and *Cd19*, respectively. Clusters 5, 9, and 12 strongly expressed *H2-Aa*. Except for Cluster 14, all clusters expressed *Ptprc* (CD45), an important marker for immune cells. Additionally, we found high expression of *Col1a1* in Cluster 14 (Supplementary Figure 3B). After preliminary analysis, we identified five tumor-associated macrophages (Cluster 0: TAM-1, Cluster 1: TAM-2, Cluster 8: TAM-3, Cluster 10: TAM4, and Cluster 11: TAM-5), two monocytes (Cluster 2:
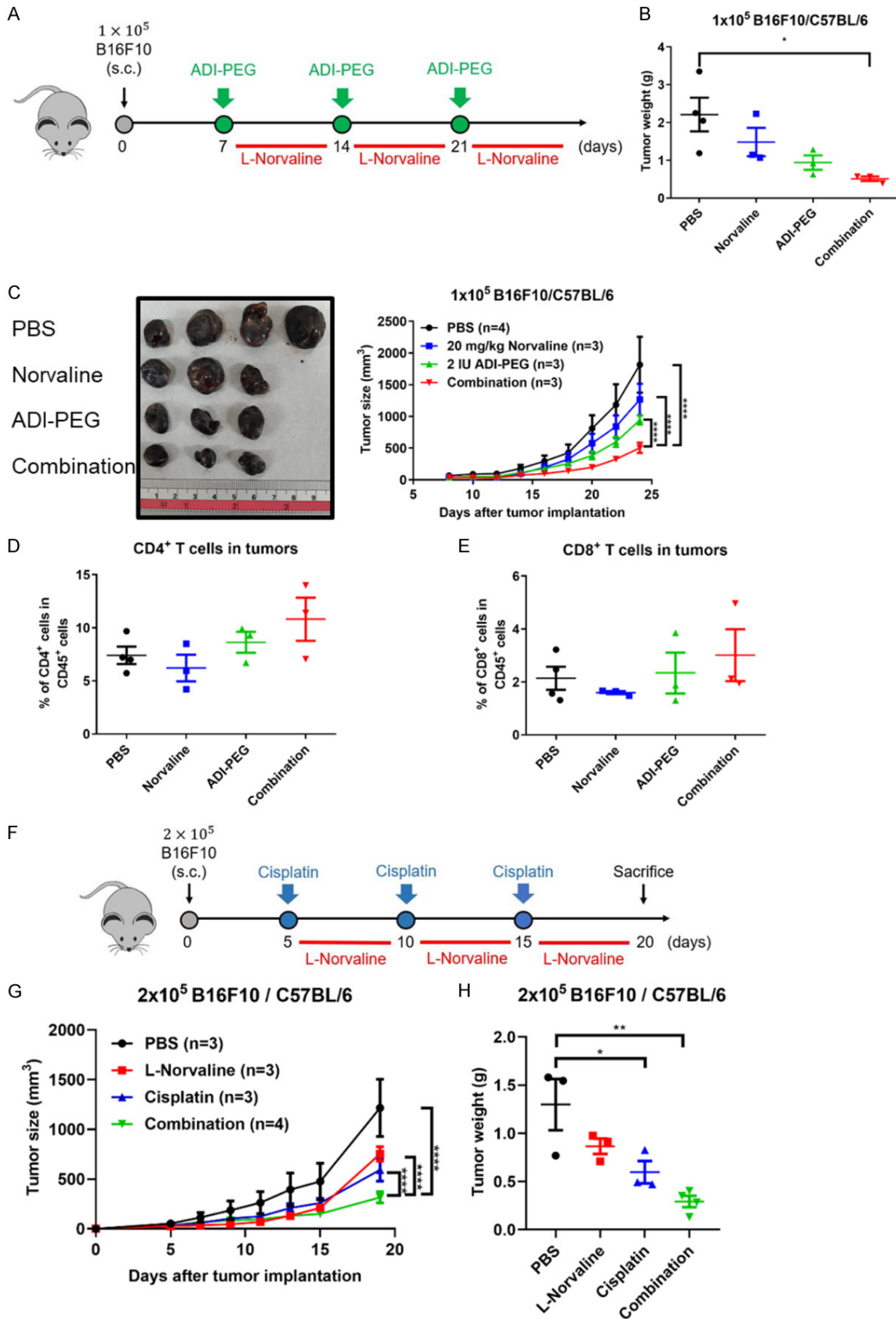
Figure 4. Combination treatment of L-Norvaline with ADI-PEG 20 or an FDA-approved drug induces an additive effect on tumor inhibition. (A) Overview of the treatment strategy: mice were subcutaneously injected with B16F10 cells.

Seven days after implantation, mice received different treatment strategies: (i) PBS, (ii) 20 mg/kg L-Norvaline, (iii) 2 IU ADI-PEG 20, and (iv) L-Norvaline and ADI-PEG 20. Mice were administered L-Norvaline once daily and intraperitoneally injected with ADI-PEG 20 once weekly. (B) Final tumor image and tumor weight of harvested tumors on Day 26. (C) Comparison of tumor size in C57BL/6 mice among the different groups. (D) The percentages of CD4$^+$ and (E) CD8$^+$ T cells among CD45$^+$CD3$^+$ cells were analyzed by flow cytometry. Tumors of treated mice were harvested on Day 26. (F) Overview of the treatment strategy: Mice were subcutaneously injected with B16F10 cells. Five days after implantation, 5 mg/kg cisplatin was administered intraperitoneally, followed by 20 mg/kg norvaline daily for four days as a treatment cycle. Mice received three treatment cycles. (G) Comparison of tumor size in C57BL/6 mice among different groups. (H) Final tumor weight of harvested tumors on Day 20. P values of the tumor curve were obtained by two-way ANOVA. P values of tumor weight were obtained by one-way ANOVA. The tumor results are presented as the means ± SEM. $^{**}P < 0.01$, $^{***}P < 0.001$, $^{***}P < 0.0001$.

Monocyte-1, and Cluster 3: Monocyte-2), three DCs (Cluster 5: Dendritic cell-1, Cluster 9: Dendritic cell-2, and Cluster 12: Dendritic cell-3), three T cells (Cluster 4: T cell-1, Cluster 6: T cell-2, and Cluster 7: T cell-3), one B cell (Cluster 13), and one fibroblast (Cluster 14). Next, we calculated and displayed the top five DEGs and marker genes in each cluster (Supplementary Figure 3C and Supplementary Data 1) for further annotation. Additionally, we identified the specific expression genes from DEGs in each cluster for cluster annotation (Supplementary Table 3), and the expression levels of specific genes were analyzed (Supplementary Figure 4). Moreover, we renamed clusters and visualized the results by uniform manifold approximation and projection (UMAP) (**Figure 5A**). To investigate whether combination treatment with L-Norvaline and ADI-PEG 20 regulated the TME, we further analyzed the alteration of each immune cell type after different treatments. Combination treatment increased six immune cells by over 1.5-fold (C0: *Mmp12*-positive macrophages, C2: *Itga5*- and *Socs3*-positive monocytes, C6: regulatory T cells, C7: cytotoxic T cells, C9: *Ccr7*-positive DCs, and C10: proliferated TAMs). Additionally, two immune cells were dramatically decreased (C3: *S100a8*- and *S100a9*-positive monocytes and C4: *Retnla*- and *Retnlg*-positive macrophages) (**Figure 5B** and **Table 1**).

Anti-tumor response observed with the combination treatment of L-Norvaline and ADI-PEG 20 is associated with an increase in Ccr7$^+$ dendritic cells and CD8$^+$ cytotoxic T cells

Previous data showed an increase in the number of infiltrated CD4$^+$ and CD8$^+$ T cells following combination treatment (**Figure 4D** and **4E**). Single-cell RNA seq data revealed a 3.49-fold increase in CD8$^+$ cytotoxic T cells after combination treatment (**Figure 5B** and **Table 1**). Flow cytometry analysis also detected an increase in the numbers of CD8$^+$ cytotoxic T cells following combination treatment, but without statistical significance (Supplementary Figure 5A).

To further understand what mechanisms were activated after the combination treatment, we performed Gene Set Enrichment Analysis (GSEA) and biological process analysis in CD8$^+$ cytotoxic T cells. The GSEA results showed that combination treatment with L-Norvaline and ADI-PEG 20 mainly upregulated cell cycle-related pathways, including the E2F target, G2/M checkpoint, and mitotic spindle (**Figure 5C**). Additionally, biological process analysis showed that most upregulated genes were involved in ribosome-related pathways, and some genes were enriched in T cells activation pathway (**Figure 5D**). Indeed, the cluster 7 (CD8$^+$ cytotoxic T cells) highly expressed the cell cycle-related gene, stathmin (*Stmn1*) (**Figure 5E**), which regulated the T-cell cytotoxicity and T-cell activation [44]. Furthermore, DCs also played an important role in the activation of CD8$^+$ cytotoxic T cells. Single-cell RNA seq data revealed that the combination treatment increased the numbers of all subsets of DCs (**Table 1**). Flow cytometry analysis also demonstrated that the total number of DCs were weakly increased in the TME following the combination treatment, but did not reach statistical significance (Supplementary Figure 5B). Importantly, single-cell RNA sequencing data demonstrated that C-C chemokine receptor type 7 (CCR7) positive DCs, an important role in regulated the CD8$^+$ T cell activation [45], were increased in the group of combination treatment. Moreover, our previous study also demonstrated that mature CCR7 positive DCs in the TME was correlated with the numbers of CD8$^+$ cytotoxic T cells and anti-tumor response following the low-dose nitric oxide donor treatment [46]. These results suggested that the anti-tumor response of the
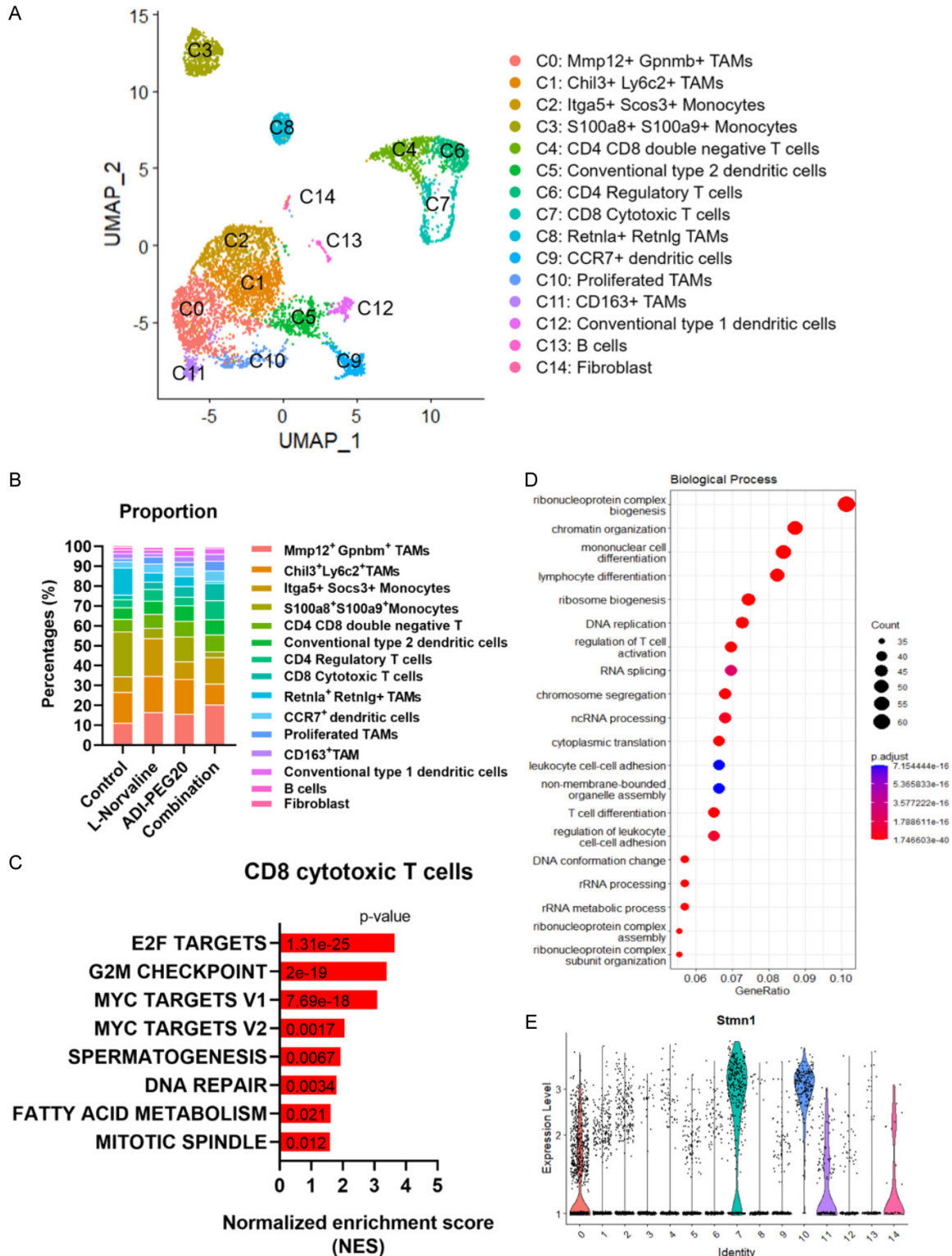
Figure 5. Combination treatment of L-Norvaline with ADI-PEG 20 induces cell-cycle-related pathways in infiltrated CD8 cytotoxic T cells. A. A total of 6485 immune cells are shown in the UMAP projection. Fifteen clusters were identified by the "Findcluster" function. Each dot plot represents one cell. B. The proportion of each cluster. C. Gene set enrichment analysis of CD8 cytotoxic T cells. All pathways had significance (*p* value < 0.05). All genes were obtained from the marker gene list, and the log2 fold change of each gene was over 0.25. D. Dot plot of CD8 cytotoxic T-cell biological processes showing the top 20 enriched pathways. A log2 fold change over 0.5 was chosen as a cutoff value. The dot size was proportional to the number of upregulated genes in the signaling. E. The expression levels of Stmn1 in each cluster. The log values were calculated.

Table 1. The alteration of immune cells population in different treatments

Clusters	Control	L-Norvaline	ADI-PEG20	Combination	Fold Change (Combination/Control)
Mmp12$^+$ Gpnmb$^+$ TAMs	11.15	16.40	15.64	20.20	1.81
Chil3$^+$ Ly6c2$^+$ TAMs	15.48	18.27	17.49	10.62	0.69
Itga5$^+$ Socs3$^+$ Mono	7.74	19.05	8.78	13.35	1.72
S100a8$^+$ S100a9$^+$ Mono	22.58	5.14	12.55	2.88	0.13
Double Negative T	6.45	6.95	7.96	8.54	1.32
cDC2	5.81	6.75	7.82	7.54	1.30
Regulatory T	3.87	5.81	4.18	9.58	2.47
Cytotoxic T	2.49	3.63	5.49	8.68	3.49
Retnla$^+$ Retnlg$^+$ TAMs	13.55	4.62	4.87	0.99	0.07
CCR7$^+$ DC	3.13	4.62	4.87	5.31	1.69
Proliferated TAMs	1.57	3.37	2.33	4.86	3.10
CD163$^+$ TAMs	2.49	1.66	2.88	3.52	1.42
cDC1	1.84	1.97	3.09	2.68	1.45
B cells	1.29	1.19	1.51	0.89	0.69
Fibroblast	0.55	0.57	0.55	0.35	0.63

combination treatment might be attributed, in part, to an increase in DCs and dendritic cell-mediated activation of CD8$^+$ cytotoxic T cells.

Reducing immunosuppressive S100a8$^+$ S100a9$^+$ monocytes and Retnla$^+$ Retnlg$^+$ TAMs was correlated with tumor regression by L-Norvaline and ADI-PEG 20 combination treatment

The combination treatment of L-Norvaline and ADI-PEG 20 resulted in a significant decrease in *Retnla$^+$ Retnlg$^+$* TAMs and *S100a8$^+$ S100a9$^+$* monocytes. However, the role of *S100a8$^+$ S100a9$^+$* monocytes in cancer progression is not fully understood yet. Therefore, we used GSEA and biological process analysis to identify potential mechanisms for the anti-tumor response of the combination treatment in *S100a8$^+$ S100a9$^+$* monocytes. Interestingly, GSEA data showed a significant downregulation in the interferon gamma response (**Figure 6A**, top). Previous studies showed that S100A9 inhibited the adaptive immune system via inhibition of antigen presentation by DCs and subsequent T-cell priming [47]. These results suggested that *S100a8$^+$ S100a9$^+$* monocytes might impede CD8$^+$ cytotoxic T cell-mediated cell killing. Furthermore, reducing the number of *S100a8$^+$ S100a9$^+$* monocytes was correlated with an anti-tumor response to the combination treatment with L-Norvaline and ADI-PEG 20. On the other hand, the up-regulated genes in *S100a8$^+$ S100a9$^+$* monocytes significantly

regulated immune cell migration, including leukocytes, myeloid cells, and granulocytes (**Figure 6A**, *bottom*). However, the role of immune cell migration in tumor progression is still unclear [48]. Therefore, further research is necessary to determine whether *S100a8$^+$ S100a9$^+$* monocytes can interfere with the anti-tumor response through immune cell migration. Additionally, *Retnla$^+$ Retnlg$^+$* TAMs showed a 13-fold decrease in the combination treatment group (**Table 1**). We further used GSEA to demonstrate its role in tumor progression. The up-regulated DEGs of *Retnla$^+$ Retnlg$^+$* TAMs were enriched in transforming growth factor-beta (TGF-β) signaling, an immunosuppressive pathway. Conversely, the down-regulated genes were enriched in interferon-gamma response (**Figure 6B**), implying that *Retnla$^+$ Retnlg$^+$* TAMs interfere with the function of CD8$^+$ cytotoxic T cells. Overall, the reduction in the number of *S100a8$^+$ S100a9$^+$* monocytes and *Retnla$^+$ Retnlg$^+$* TAMs in the TME was found to be correlated with an additive effect on the anti-tumor response of the combination treatment with L-Norvaline and ADI-PEG 20.

To summarize, the administration of L-Norvaline had an anti-tumor effect by regulating immune signaling in tumor cells and the complete immune system. Furthermore, the combination treatment of L-Norvaline and ADI-PEG 20 exhibited an additive effect in tumor destruction and modulated the TME from an immunosuppressive state to an immunoreactive state. This
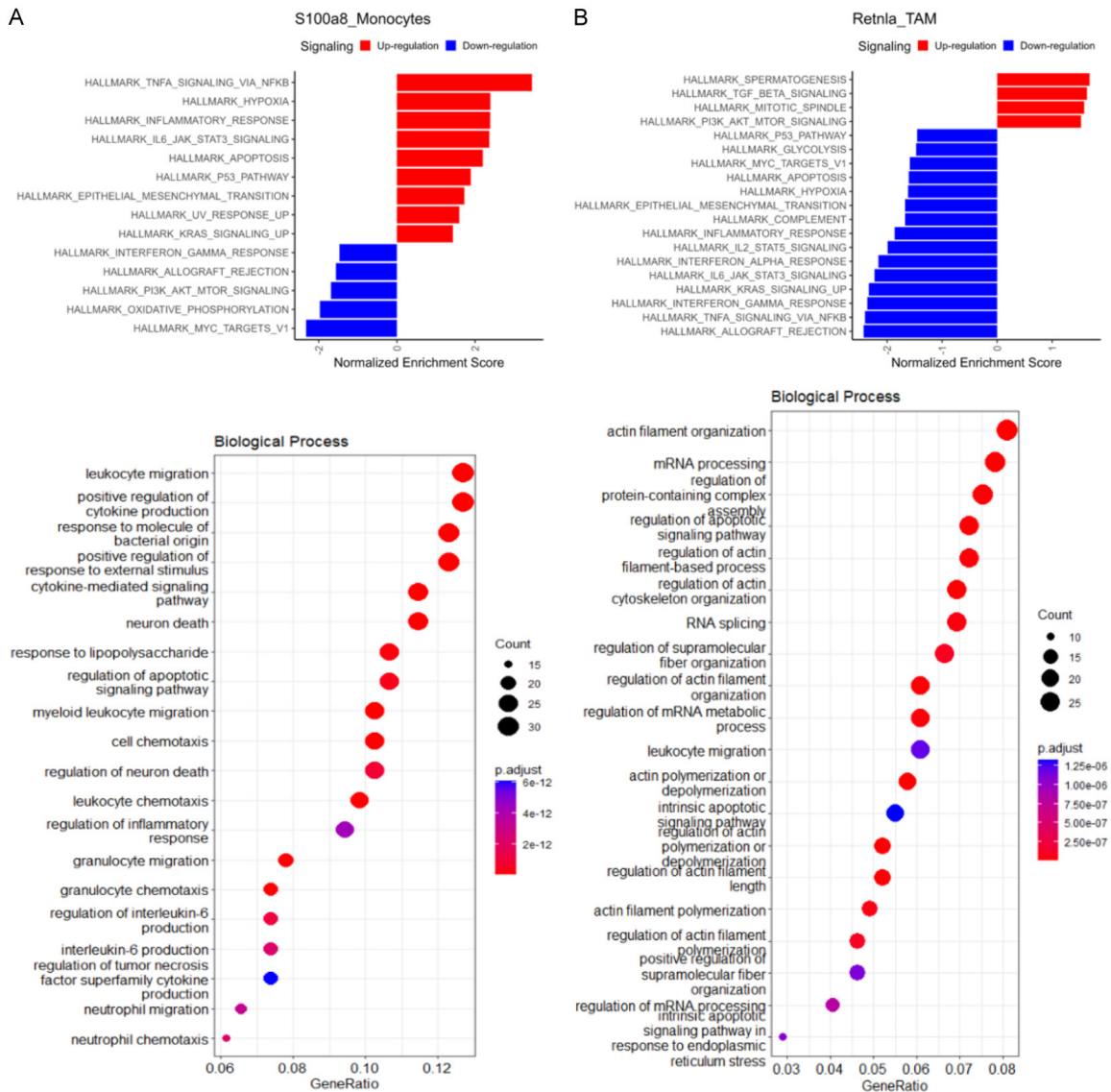
Figure 6. *S100a8+ S100a9+* monocytes and *Retnla+ Retnlg+* TAMs down-regulate interferon gamma response and mediate leukocyte migration in the TME. (A) Hallmark gene set analysis and biological process analysis of significant genes in *S100a8+ S100a9+* monocytes and (B) *Retnla+ Retnlg+* TAMs. A log2 fold-change over 0.5 was chosen as a cut-off value in biological process analysis. Dot size was proportional to the number of up-regulated genes in the signaling. The significant genes were identified by the "FindMarker" function in the Seurat package. All pathways have significance (*p* value < 0.05).

modulation was achieved by altering the proportions of *Retnla+ Retnlg+* TAMs, *S100a8+ S100a9+* monocytes, *Ccr7+* DCs, and CD8+ cytotoxic T cells. Additionally, the combination treatment promoted the proliferation and cell cycle progression of CD8+ cytotoxic T cells.

Discussion

Arginase has been described as an immunosuppressive regulator in tumors. Tumors that express high levels of arginase tend to have worse clinical outcomes in patients. Accordingly, arginase is an attractive target for anticancer agent development. Indeed, several arginase inhibitors have been reported to effectively reduce tumor development. However, the role of L-Norvaline in tumorigenesis has been less investigated. Our research is in accordance with previous findings suggesting that blocking arginase activity restrains tumor growth. In the present study, we found that 20 mg/kg

L-Norvaline could inhibit the growth of B16F10 melanoma and LL2 Lewis lung carcinoma and that the anticancer responses of L-Norvaline required complete immunity. In addition, our findings suggest that L-Norvaline enhance cancer therapeutics when combined with ADI-PEG 20, indicating its potential as an immunomodulator for cancer treatment. Moreover, it is important to note that L-Norvaline is a dietary supplement and it decreases cell viability in mammalian cells even at concentrations higher than 125 µM [49]. Interestingly, our in vitro data showed that L-Norvaline had no cytotoxic effect on tumor cells at concentrations lower than 100 µM (data not shown). Although L-Norvaline does not kill tumor cells directly, it may induce the anticancer immune response by alteration of the tumor immune microenvironment and immune-related pathways of tumor cells themselves. Indeed, KEGG and MetaCore pathway analyses suggested that DEGs of two cultured tumor cell lines, B16F10 and LL2, in response to L-Norvaline were enriched in many immune-related pathways. To further investigate whether the anti-tumor responses of L-Norvaline were partially mediated by specific tumor genes, the number of overlapping upregulated genes was narrowed (i.e., to fold changes (Nor/Ctrl) more than or equal to 2.0). Only 29 genes were upregulated in both B16F10 and LL2 cells treated with L-Norvaline. TNFSF18 (GITRL) is one such gene and is related to the immune response. TNFSF18 is a transmembrane protein and is expressed by some types of tumors or released in soluble form. Previous studies suggested that TNFSF18 expression in tumor cells inhibits cancer development and promotes the accumulation of CD8$^+$ T cells [50]. Hence, it was supposed that the anti-tumor response of L-Norvaline might partially depend on TNFSF18.

Arginine is extremely vital for T cell proliferation and activation, and thus, concerns are made for the impact to tumor immunity when environmental arginine is modulated. Our single-cell RNA-seq data revealed that combined treatment of L-Norvaline and ADI-PEG 20 promoted tumor infiltration of CD8$^+$ cytotoxic T cells, which were also suggested having proliferative potential by the upregulated *Mki67* (Ki67) gene. This is in agreement with several studies that inhibition of arginase activity would promote the accumulation of tumor-infiltrating T cells [51-53]. In our data, enhanced ribosome

biogenesis and ribonucleoprotein complex biogenesis was noted in CD8$^+$ cytotoxic T cell. Ribosome biogenesis is frequently regulated by methyltransferases, such as protein arginine methyltransferase 3 [54] and RNA cap methyltransferase (RNMT). Remarkably, RNMT was upregulated during T-cell activation [55]. However, whether a high arginine concentration induces CD8$^+$ cytotoxic T-cell activation via methyltransferase-mediated ribosome biogenesis is unknown. Notably, another regulator of ribosome biogenesis [56], protein arginine methyltransferase 5 (PRMT5), modulates T-cell proliferation, survival, and differentiation [57]. Our results and these studies implied that methyltransferases that regulate ribosome biogenesis might modulate CD8$^+$ cytotoxic T cells during combination treatment with L-Norvaline and ADI-PEG 20.

It was reported that T cells are able to regenerate endogenous arginine from recycled citrulline, the by-product of ADI-PEG 20 [58], ADI-PEG 20 treatment consumed arginine and then produced numerous citrulline in plasma [59], retaining CD8$^+$ T cells. Interestingly, we found regulatory T cells were also increased for 2.47-fold more than the control group during combination treatment. This is in accordance with the finding that suggested exogenous citrulline to induce regulatory T cells differentiation and increased cytokines production, such as IL-10 and TGF-β, which were essential for the anti-inflammatory response [60]. Additional strategy to combine with anti-CTLA4 antibodies to mitigate regulatory T cells is expected to promote anti-tumor response [61].

The anti-tumor immune responses were very complicated. Immune cells usually include multiple subsets of cells with distinctive phenotypic and functional properties. The total clusters identified based on some specific cell markers were not thorough enough. Although single-cell RNA-seq analysis revealed that the combination of L-Norvaline and ADI-PEG 20 induced significant changes in some types of tumor-infiltrating immune cells, the major cause of tumor growth inhibition awaits further investigation. Furthermore, experiments should be undertaken to determine the underlying mechanisms.

Combination therapy with L-Norvaline and ADI-PEG 20 regulated T cells and significantly decreased resistin-expressing macrophages.

Resistin is an adipokine secreted from macrophages that regulates inflammation and immune diseases. A previous study indicated that resistin inhibited neuronal autophagy through Toll-like receptor 4 [62]. Autophagy is an important mechanism for cancer cell survival. Notably, ADI-PEG 20 treatment drove arginine turnover and systemic autophagy to dictate energy metabolism [63]. Additionally, ADI-PEG 20 induced cytotoxic autophagy in ASS1-deficient prostate cancer cells [64]. These studies and our results implied that combination treatment with L-Norvaline and ADI-PEG 20 might further enhance the anti-tumor effect through autophagy improvement.

To the best of our knowledge, this is the first study to demonstrate the effect of a combination of arginase and arginine deiminase treatment on immune alterations and tumor progression.

Methods

Cell culture

B16F10 cells were maintained in Dulbecco's modified Eagle's medium with high glucose (HyClone), and LL2 cells were maintained in Dulbecco's modified Eagle's medium with low glucose (HyClone). DMEM was supplemented with 10% fetal bovine serum (NQBB) and 1% penicillin-streptomycin (HyClone). All cells were cultured at 37°C in a 5% CO_2 atmosphere.

Xenogeneic tumor model

Female seven- to eight-week-old C57BL/6 mice and six-week-old NOD/SCID mice were purchased from the Laboratory Animal Center, National Cheng Kung University (NCKU). A total of 1×10^5 B16F10 and 2×10^5 LL2 cancer cells were suspended in 100 μL serum-free high- or low-glucose DMEM and were subcutaneously injected into the right hind flanks of C57BL/6 or NOD/SCID mice. Mice were randomly grouped for experiments 5 days after tumor injection. L-Norvaline was purchased from Sigma and dissolved in 1 × PBS. Mice were given a daily intraperitoneal administration of L-Norvaline (20 or 100 mg/kg body weight) or vehicle control. ADI-PEG 20 was obtained from Dr. Kwang-Yu Chang. For the experiment of arginase inhibition combined with ADI-PEG 20 (Polaris Pharmaceuticals) treatment, ADI-PEG 20 (2 IU/mouse) was injected intraperitoneally on Days

7, 14 and 21 after tumor implantation. For the experiment of arginase inhibition combined with cisplatin (Fresenius Kabi) treatment, cisplatin (5 mg/kg body weight) was injected intraperitoneally on Days 5, 10 and 15 after tumor implantation. The tumor volumes were measured with a caliper and obtained using the formula volume = Length × Width^2 × 0.52. Tumor size and body weight were recorded every two days.

Flow cytometry analysis of tumor immune microenvironment

Tumors were harvested and minced into fine pieces in serum-free medium containing 100 IU/ml DNase I (Roche) and 1 mg/mL Collagenase A (Sigma). The samples were incubated for 1 hour under shaking (150 rpm) at 37°C, filtered through a 70 μM cell strainer, hemolyzed in RBC lysis buffer at room temperature for 5 minutes, and washed twice with flow staining buffer (FBS). Next, the cells were suspended in stain buffer and filtered through a 35 μM mesh strainer. The collected cells were then stained with Fc Block (BD Pharmingen) on ice for 15 minutes, and the following fluorescently labeled antibodies were used on ice for 30 minutes in the dark: anti-CD45-BV510, anti-CD4-APC, anti-CD8-BV510, anti-CD8-APC, anti-CD107-BV421, and anti-CD11C-BV421 (all from BD Pharmingen). The stained cells were analyzed by a flow cytometer (CytoFLEX, Beckman Coulter).

RNA isolation and bulk sequencing of murine cancer cell lines

Cancer cells were seeded in a 6 cm plate at 1×10^4 per well, cultured at 37°C for 16-18 hours, and then treated with L-Norvaline-mixed complete medium for 72 hours. Total RNA was isolated from cell pellets using TRIzol reagent (CyrusBioscience). A TruSeq Stranded mRNA Library Prep Kit (Illumina, San Diego, CA, USA) was used for library construction. An Agilent Bioanalyzer 2100 and real-time PCR were used to check the quality of the libraries. The libraries were sequenced on an Illumina NovaSeq 6000 platform with 150 bp paired-end reads. These services were provided by Genomics BioSci & Tech Co., Ltd. (New Taipei City, Taiwan). Clean data were obtained from Genomics BioSci & Tech Co., Ltd. (New Taipei City, Taiwan). Trimmomatic (version 0.39) was used to filter

raw data by removing adapter sequences and low-quality bases. In the gene expression list, a fold change (L-Norvaline/control) ≥ 1.5 or ≤ 0.5 was the criterion for significantly differentially expressed genes. To gain insight into L-Norvaline-mediated pathways in tumor cells, the pathway analysis platforms KEGG (Kyoto Encyclopedia of Genes and Genomes) and MetaCore™ (GeneGo Inc., St. Joseph, MI, USA) were used.

Murine tumor sample processing and single-cell RNA sequencing

Subcutaneous tumors were harvested using forceps and scissors and minced into fine pieces in serum-free medium containing 100 IU/ml DNase I (Roche) and 1 mg/ml Collagenase A (Sigma). The samples were incubated for 1 hour under shaking (150 rpm) at 37°C, filtered through a 70 μM cell strainer, hemolyzed in RBC lysis buffer at room temperature for 5 minutes, and washed twice with flow staining buffer. Next, the cells were suspended in flow staining buffer and filtered through a 35 μM mesh strainer. The collected cells were then stained with Fc Block at room temperature for 10 minutes and colabeled with sample tags (one sample tag per treatment group) and CD45-BV510 antibody (all from BD Pharmingen). Finally, the cells were stained with 7-aminoactinomycin D (7-AAD). Viable immune cells were sorted by a BD FACSAria™ instrument. Only CD45$^+$ 7-AAD$^-$ cells were sorted into receiving tubes containing cold sample buffer (BD Pharmingen; Cat. No. 650000062).

Viable immune cells sorted from each treatment group were stained with Calcein AM and Draq7 (Thermo) to determine the precise cell concentration and viability using a BD Rhapsody™ Scanner. The cell viability ranged from 85% to 90%. The BD Rhapsody Express system was used for single-cell transcriptomic capture based on Fan et al. All samples were pooled together and then loaded onto a BD Rhapsody™ Cartridge. Next, cell capture beads (BD Pharmingen; Cat. No. 650000089) were loaded onto the cartridge. According to the manufacturer's protocol, cells were lysed, and cell capture beads were retrieved and washed. Then, reverse transcription was performed and treated with exonuclease I (Cat. No. 650000072). Transcriptome and sample tag information of single cells were obtained from

the BD Rhapsody System. The cDNA library and sample tag library were established from micro-bead-captured single-cell transcriptome and sample tag sequences, respectively. The library construction and library sequencing were performed by the Institute of Molecular and Genomic Medicine of the National Health Research Institute, and the single-cell library was analyzed with the NovaSeq 6000 system.

Bioinformatics and computational biology analyses

Raw data were aligned to the mouse genome (GRCm38.p6, gencode M19), and transcriptomic information was produced by Rhapsody WTA pipeline V1.9. The control group had 1223 cells, the L-Norvaline group had 2134 cells, the ADI-PEG 20 group had 1637 cells, and the combination group had 2350 cells for analysis. We analyzed the count matrix via Seurat (Version 4.0.5) [65]. Genes and cells were removed by the following conditions: cells with less than 200 feature genes and 25% mitochondrial gene expression. In total, we obtained 6485 cells (control: 1085, L-Norvaline: 1927, ADI-PEG: 1458, combination: 2015). The Seurat function "normalize Data" was used to normalize the raw count data, and the normalized method was log normalization. Variable genes were found by the "FindVariableFeatures" function. Default parameters were used for the Seurat function. Clusters were identified by the "FindClusters" function. The dimensions of the data were reduced through uniform manifold approximation and projection (UMAP). The significant genes in each cluster were identified via the "FindMarkers" function. If the values of log2 fold change (log2FC) were lower than 0.25, these genes were removed from the gene list. Biological process (BP) and Kyoto Encyclopedia of Genes and Genomes (KEGG) analyses were performed using the "ClusterProfiler" package. Additionally, gene set enrichment analysis (GSEA) was performed by the "fgsea" package in R. We selected hallmark gene set databases from GSEA for our analysis.

Statistical analysis

Graphic representation and statistical calculations were conducted using GraphPad Prism version 8 (La Jolla, CA, USA). All data are shown as the mean ± standard error of the mean (SEM). Statistical significance was determined

by t-test or one- and two-way ANOVA. Figures marked with asterisks indicate that the differences between groups were statistically significant.

Disclosure of conflict of interest

None.

Address correspondence to: Dr. Ming-Derg Lai, Department of Biochemistry and Molecular Biology, College of Medicine, National Cheng Kung University, No. 1, University Road, Tainan 701, Taiwan, ROC. Tel: +886-6-2353535 Ext. 5549; Fax: +886-6-2741694; E-mail: a1211207@mail.ncku.edu.tw; Dr. Kwang-Yu Chang, National Institute of Cancer Research, National Health Research Institutes, No. 367, Sheng Li Road, Tainan 704, Taiwan, ROC. Tel: +886-6-7000123 Ext. 65112; E-mail: kwang2@nhri.edu.tw

References

[1] Waldman AD, Fritz JM and Lenardo MJ. A guide to cancer immunotherapy: from T cell basic science to clinical practice. Nat Rev Immunol 2020; 20: 651-668.

[2] Larkin J, Chiarion-Sileni V, Gonzalez R, Grob JJ, Cowey CL, Lao CD, Schadendorf D, Dummer R, Smylie M, Rutkowski P, Ferrucci PF, Hill A, Wagstaff J, Carlino MS, Haanen JB, Maio M, Marquez-Rodas I, McArthur GA, Ascierto PA, Long GV, Callahan MK, Postow MA, Grossmann K, Sznol M, Dreno B, Bastholt L, Yang A, Rollin LM, Horak C, Hodi FS and Wolchok JD. Combined nivolumab and ipilimumab or monotherapy in untreated melanoma. N Engl J Med 2015; 373: 23-34.

[3] Beatty GL and Gladney WL. Immune escape mechanisms as a guide for cancer immunotherapy. Clin Cancer Res 2015; 21: 687-692.

[4] Yen MC, Lin CC, Chen YL, Huang SS, Yang HJ, Chang CP, Lei HY and Lai MD. A novel cancer therapy by skin delivery of indoleamine 2,3-dioxygenase siRNA. Clin Cancer Res 2009; 15: 641-649.

[5] Rodriguez PC, Ochoa AC and Al-Khami AA. Arginine metabolism in myeloid cells shapes innate and adaptive immunity. Front Immunol 2017; 8: 93.

[6] Érsek B, Silló P, Cakir U, Molnár V, Bencsik A, Mayer B, Mezey E, Kárpáti S, Pós Z and Németh K. Melanoma-associated fibroblasts impair CD8+ T cell function and modify expression of immune checkpoint regulators via increased arginase activity. Cell Mol Life Sci 2021; 78: 661-673.

[7] Wang CY, Chiao CC, Phan NN, Li CY, Sun ZD, Jiang JZ, Hung JH, Chen YL, Yen MC, Weng TY, Chen WC, Hsu HP and Lai MD. Gene signatures and potential therapeutic targets of amino acid metabolism in estrogen receptor-positive breast cancer. Am J Cancer Res 2020; 10: 95-113.

[8] Geiger R, Rieckmann JC, Wolf T, Basso C, Feng Y, Fuhrer T, Kogadeeva M, Picotti P, Meissner F, Mann M, Zamboni N, Sallusto F and Lanzavecchia A. L-Arginine modulates T cell metabolism and enhances survival and anti-tumor activity. Cell 2016; 167: 829-842, e13.

[9] Rodriguez PC, Zea AH, DeSalvo J, Culotta KS, Zabaleta J, Quiceno DG, Ochoa JB and Ochoa AC. L-arginine consumption by macrophages modulates the expression of CD3 zeta chain in T lymphocytes. J Immunol 2003; 171: 1232-1239.

[10] Baniyash M. TCR zeta-chain downregulation: curtailing an excessive inflammatory immune response. Nat Rev Immunol 2004; 4: 675-687.

[11] Rodriguez PC, Quiceno DG and Ochoa AC. L-arginine availability regulates T-lymphocyte cell-cycle progression. Blood 2007; 109: 1568-1573.

[12] Chen CL, Hsu SC, Ann DK, Yen Y and Kung HJ. Arginine signaling and cancer metabolism. Cancers (Basel) 2021; 13: 3541.

[13] Arlauckas SP, Garren SB, Garris CS, Kohler RH, Oh J, Pittet MJ and Weissleder R. Arg1 expression defines immunosuppressive subsets of tumor-associated macrophages. Theranostics 2018; 8: 5842-5854.

[14] Grzywa TM, Sosnowska A, Matryba P, Rydzynska Z, Jasinski M, Nowis D and Golab J. Myeloid cell-derived arginase in cancer immune response. Front Immunol 2020; 11: 938-938.

[15] Dunand-Sauthier I, Irla M, Carnesecchi S, Seguín-Estévez Q, Vejnar CE, Zdobnov EM, Santiago-Raber ML and Reith W. Repression of arginase-2 expression in dendritic cells by microRNA-155 is critical for promoting T cell proliferation. J Immunol 2014; 193: 1690-1700.

[16] Lowe MM, Boothby I, Clancy S, Ahn RS, Liao W, Nguyen DN, Schumann K, Marson A, Mahuron

KM, Kingsbury GA, Liu Z, Munoz Sandoval P, Rodriguez RS, Pauli ML, Taravati K, Arron ST, Neuhaus IM, Harris HW, Kim EA, Shin US, Krummel MF, Daud A, Scharschmidt TC and Rosenblum MD. Regulatory T cells use arginase 2 to enhance their metabolic fitness in tissues. JCI Insight 2019; 4: e129756.

[17] Martí i Líndez AA, Dunand-Sauthier I, Conti M, Gobet F, Núñez N, Hannich JT, Riezman H, Geiger R, Piersigilli A, Hahn K, Lemeille S, Becher B, De Smedt T, Hugues S and Reith W. Mitochondrial arginase-2 is a cell-autonomous regulator of CD8+ T cell function and antitumor efficacy. JCI Insight 2019; 4: e132975.

[18] Süer Gökmen S, Yörük Y, Cakir E, Yorulmaz F and Gülen S. Arginase and ornithine, as markers in human non-small cell lung carcinoma. Cancer Biochem Biophys 1999; 17: 125-131.

[19] Graboń W, Mielczarek-Puta M, Chrzanowska A and Barańczyk-Kuźma A. L-arginine as a factor increasing arginase significance in diagnosis of primary and metastatic colorectal cancer. Clin Biochem 2009; 42: 353-357.

[20] de Boniface J, Mao Y, Schmidt-Mende J, Kiessling R and Poschke I. Expression patterns of the immunomodulatory enzyme arginase 1 in blood, lymph nodes and tumor tissue of early-stage breast cancer patients. Oncoimmunology 2012; 1: 1305-1312.

[21] Gökmen SS, Aygit AC, Ayhan MS, Yorulmaz F and Gülen S. Significance of arginase and ornithine in malignant tumors of the human skin. J Lab Clin Med 2001; 137: 340-344.

[22] Coosemans A, Decoene J, Baert T, Laenen A, Kasran A, Verschuere T, Seys S and Vergote I. Immunosuppressive parameters in serum of ovarian cancer patients change during the disease course. Oncoimmunology 2016; 5: e1111505.

[23] Czystowska-Kuzmicz M, Sosnowska A, Nowis D, Ramji K, Szajnik M, Chlebowska-Tuz J, Wolinska E, Gaj P, Grazul M, Pilch Z, Zerrouqi A, Graczyk-Jarzynka A, Soroczynska K, Cierniak S, Koktysz R, Elishaev E, Gruca S, Stefanowicz A, Blaszczyk R, Borek B, Gzik A, Whiteside T and Golab J. Small extracellular vesicles containing arginase-1 suppress T-cell responses and promote tumor growth in ovarian carcinoma. Nat Commun 2019; 10: 3000.

[24] Pudlo M, Demougeot C and Girard-Thernier C. Arginase inhibitors: a rational approach over one century. Med Res Rev 2017; 37: 475-513.

[25] Rodriguez PC, Quiceno DG, Zabaleta J, Ortiz B, Zea AH, Piazuelo MB, Delgado A, Correa P, Brayer J, Sotomayor EM, Antonia S, Ochoa JB and Ochoa AC. Arginase I production in the tumor microenvironment by mature myeloid cells inhibits T-cell receptor expression and antigen-specific T-cell responses. Cancer Res 2004; 64: 5839-5849.

[26] Miret JJ, Kirschmeier P, Koyama S, Zhu M, Li YY, Naito Y, Wu M, Malladi VS, Huang W, Walker W, Palakurthi S, Dranoff G, Hammerman PS, Pecot CV, Wong KK and Akbay EA. Suppression of myeloid cell arginase activity leads to therapeutic response in a NSCLC mouse model by activating anti-tumor immunity. J Immunother Cancer 2019; 7: 32.

[27] Polis B, Srikanth KD, Elliott E, Gil-Henn H and Samson AO. L-norvaline reverses cognitive decline and synaptic loss in a murine model of Alzheimer's disease. Neurotherapeutics 2018; 15: 1036-1054.

[28] Gao L, Zhang JH, Chen XX, Ren HL, Feng XL, Wang JL and Xiao JH. Combination of L-arginine and L-norvaline protects against pulmonary fibrosis progression induced by bleomycin in mice. Biomed Pharmacother 2019; 113: 108768.

[29] Javrushyan H, Nadiryan E, Grigoryan A, Avtandilyan N and Maloyan A. Antihyperglycemic activity of L-norvaline and L-arginine in high-fat diet and streptozotocin-treated male rats. Exp Mol Pathol 2022; 126: 104763.

[30] Gilinsky MA, Polityko YK, Markel AL, Latysheva TV, Samson AO, Polis B and Naumenko SE. Norvaline reduces blood pressure and induces diuresis in rats with inherited stress-induced arterial hypertension. Biomed Res Int 2020; 2020: 4935386.

[31] Polis B, Srikanth KD, Gurevich V, Gil-Henn H and Samson AO. L-norvaline, a new therapeutic agent against Alzheimer's disease. Neural Regen Res 2019; 14: 1562-1572.

[32] Polis B, Gurevich V, Assa M and Samson AO. Norvaline restores the BBB integrity in a mouse model of Alzheimer's disease. Int J Mol Sci 2019; 20: 4616.

[33] Alexandrou C, Al-Aqbi SS, Higgins JA, Boyle W, Karmokar A, Andreadi C, Luo JL, Moore DA, Viskaduraki M, Blades M, Murray GI, Howells LM, Thomas A, Brown K, Cheng PN and Rufini A. Sensitivity of colorectal cancer to arginine deprivation therapy is shaped by differential expression of urea cycle enzymes. Sci Rep 2018; 8: 12096.

[34] Feun L, You M, Wu CJ, Kuo MT, Wangpaichitr M, Spector S and Savaraj N. Arginine deprivation as a targeted therapy for cancer. Curr Pharm Des 2008; 14: 1049-1057.

[35] Ensor CM, Holtsberg FW, Bomalaski JS and Clark MA. Pegylated arginine deiminase (ADI-SS PEG20,000 mw) inhibits human melanomas and hepatocellular carcinomas in vitro and in vivo. Cancer Res 2002; 62: 5443-5450.

[36] Feun LG, Marini A, Walker G, Elgart G, Moffat F, Rodgers SE, Wu CJ, You M, Wangpaichitr M,

Kuo MT, Sisson W, Jungbluth AA, Bomalaski J and Savaraj N. Negative argininosuccinate synthetase expression in melanoma tumours may predict clinical benefit from arginine-depleting therapy with pegylated arginine deiminase. Br J Cancer 2012; 106: 1481-1485.

[37] Harding JJ, Do RK, Dika IE, Hollywood E, Uhlitskykh K, Valentino E, Wan P, Hamilton C, Feng X, Johnston A, Bomalaski J, Li CF, O'Reilly EM and Abou-Alfa GK. A phase 1 study of ADI-PEG 20 and modified FOLFOX6 in patients with advanced hepatocellular carcinoma and other gastrointestinal malignancies. Cancer Chemother Pharmacol 2018; 82: 429-440.

[38] Lowery MA, Yu KH, Kelsen DP, Harding JJ, Bomalaski JS, Glassman DC, Covington CM, Brenner R, Hollywood E, Barba A, Johnston A, Liu KC, Feng X, Capanu M, Abou-Alfa GK and O'Reilly EM. A phase 1/1B trial of ADI-PEG 20 plus nab-paclitaxel and gemcitabine in patients with advanced pancreatic adenocarcinoma. Cancer 2017; 123: 4556-4565.

[39] Brin E, Wu K, Lu HT, He Y, Dai Z and He W. PEGylated arginine deiminase can modulate tumor immune microenvironment by affecting immune checkpoint expression, decreasing regulatory T cell accumulation and inducing tumor T cell infiltration. Oncotarget 2017; 8: 58948-58963.

[40] Chang KY, Chiang NJ, Wu SY, Yen CJ, Chen SH, Yeh YM, Li CF, Feng X, Wu K, Johnston A, Bomalaski JS, Wu BW, Gao J, Subudhi SK, Kaseb AO, Blando JM, Yadav SS, Szlosarek PW and Chen LT. Phase 1b study of pegylated arginine deiminase (ADI-PEG 20) plus Pembrolizumab in advanced solid cancers. Oncoimmunology 2021; 10: 1943253.

[41] Szlosarek PW, Phillips MM, Pavlyk I, Steele J, Shamash J, Spicer J, Kumar S, Pacey S, Feng X, Johnston A, Bomalaski J, Moir G, Lau K, Ellis S and Sheaff M. Expansion phase 1 study of pegargiminase plus pemetrexed and cisplatin in patients with argininosuccinate synthetase 1-deficient mesothelioma: safety, efficacy, and resistance mechanisms. JTO Clin Res Rep 2020; 1: 100093.

[42] Galluzzi L, Buqué A, Kepp O, Zitvogel L and Kroemer G. Immunological effects of conventional chemotherapy and targeted anticancer agents. Cancer Cell 2015; 28: 690-714.

[43] de Biasi AR, Villena-Vargas J and Adusumilli PS. Cisplatin-induced antitumor immunomodulation: a review of preclinical and clinical evidence. Clin Cancer Res 2014; 20: 5384-5391.

[44] Filbert EL, Le Borgne M, Lin J, Heuser JE and Shaw AS. Stathmin regulates microtubule dynamics and microtubule organizing center polarization in activated T cells. J Immunol 2012; 188: 5421-5427.

[45] Roberts EW, Broz ML, Binnewies M, Headley MB, Nelson AE, Wolf DM, Kaisho T, Bogunovic D, Bhardwaj N and Krummel MF. Critical role for CD103(+)/CD141(+) dendritic cells bearing CCR7 for tumor antigen trafficking and priming of T cell immunity in melanoma. Cancer Cell 2016; 30: 324-336.

[46] Li CY, Anuraga G, Chang CP, Weng TY, Hsu HP, Ta HDK, Su PF, Chiu PH, Yang SJ, Chen FW, Ye PH, Wang CY and Lai MD. Repurposing nitric oxide donating drugs in cancer therapy through immune modulation. J Exp Clin Cancer Res 2023; 42: 22.

[47] Shimizu K, Libby P, Rocha VZ, Folco EJ, Shubiki R, Grabie N, Jang S, Lichtman AH, Shimizu A, Hogg N, Simon DI, Mitchell RN and Croce K. Loss of myeloid related protein-8/14 exacerbates cardiac allograft rejection. Circulation 2011; 124: 2920-2932.

[48] Shelton SE, Nguyen HT, Barbie DA and Kamm RD. Engineering approaches for studying immune-tumor cell interactions and immunotherapy. iScience 2020; 24: 101985.

[49] Samardzic K and Rodgers KJ. Cytotoxicity and mitochondrial dysfunction caused by the dietary supplement l-norvaline. Toxicol In Vitro 2019; 56: 163-171.

[50] Cho JS, Hsu JV and Morrison SL. Localized expression of GITR-L in the tumor microenvironment promotes CD8+ T cell dependent antitumor immunity. Cancer Immunol Immunother 2009; 58: 1057-1069.

[51] Sosnowska A, Chlebowska-Tuz J, Matryba P, Pilch Z, Greig A, Wolny A, Grzywa TM, Rydzynska Z, Sokolowska O, Rygiel TP, Grzybowski M, Stanczak P, Blaszczyk R, Nowis D and Golab J. Inhibition of arginase modulates T-cell response in the tumor microenvironment of lung carcinoma. Oncoimmunology 2021; 10: 1956143.

[52] Steggerda SM, Bennett MK, Chen J, Emberley E, Huang T, Janes JR, Li W, MacKinnon AL, Makkouk A, Marguier G, Murray PJ, Neou S, Pan A, Parlati F, Rodriguez MLM, Van de Velde LA, Wang T, Works M, Zhang J, Zhang W and Gross MI. Inhibition of arginase by CB-1158 blocks myeloid cell-mediated immune suppression in the tumor microenvironment. J Immunother Cancer 2017; 5: 101.

[53] Schuller A, Doshi A, Cantin S, Secinaro M, Wang Y, Prickett L, Tentarelli S, Gangl E, Ghadially H, Ilieva K, Proia T, Mlynarski S, Finlay R and Shao W. Abstract 4523: inhibition of arginase in combination with anti-PDL1 leads to increased infiltration and activation of CD8+ T cells, NK cells, and CD103+ dendritic cells in mouse syngeneic tumor models. Cancer Res 2020; 80: 4523.

[54] Hang R, Liu C, Ahmad A, Zhang Y, Lu F and Cao X. Arabidopsis protein arginine methyltransferase 3 is required for ribosome biogenesis by affecting precursor ribosomal RNA processing. Proc Natl Acad Sci U S A 2014; 111: 16190-16195.

[55] Galloway A, Kaskar A, Ditsova D, Atrih A, Yoshikawa H, Gomez-Moreira C, Suska O, Warminski M, Grzela R, Lamond AI, Darzynkiewicz E, Jemielity J and Cowling Victoria H. Upregulation of RNA cap methyltransferase RNMT drives ribosome biogenesis during T cell activation. Nucleic Acids Res 2021; 49: 6722-6738.

[56] Ren J, Wang Y, Liang Y, Zhang Y, Bao S and Xu Z. Methylation of ribosomal protein S10 by protein-arginine methyltransferase 5 regulates ribosome biogenesis. J Biol Chem 2010; 285: 12695-12705.

[57] Sengupta S, Kennemer A, Patrick K, Tsichlis P and Guerau-de-Arellano M. Protein arginine methyltransferase 5 in T lymphocyte biology. Trends Immunol 2020; 41: 918-931.

[58] Werner A, Koschke M, Leuchtner N, Luckner-Minden C, Habermeier A, Rupp J, Heinrich C, Conradi R, Closs EI and Munder M. Reconstitution of T cell proliferation under arginine limitation: activated human T cells take up citrulline via L-type amino acid transporter 1 and use it to regenerate arginine after induction of argininosuccinate synthase expression. Front Immunol 2017; 8: 864.

[59] Yuan Y, Mohammad MA, Betancourt A, Didelija IC, Yallampalli C and Marini JC. The citrulline recycling pathway sustains cardiovascular function in arginine-depleted healthy mice, but cannot sustain nitric oxide production during endotoxin challenge. J Nutr 2018; 148: 844-850.

[60] Lee YC, Su YT, Liu TY, Tsai CM, Chang CH and Yu HR. L-arginine and L-citrulline supplementation have different programming effect on regulatory T-cells function of infantile rats. Front Immunol 2018; 9: 2911.

[61] Togashi Y, Shitara K and Nishikawa H. Regulatory T cells in cancer immunosuppression - implications for anticancer therapy. Nat Rev Clin Oncol 2019; 16: 356-371.

[62] Miao J, Benomar Y, Al Rifai S, Poizat G, Riffault L, Crépin D and Taouis M. Resistin inhibits neuronal autophagy through Toll-like receptor 4. J Endocrinol 2018; 238: 77-89.

[63] Zhang Y, Higgins CB, Van Tine BA, Bomalaski JS and DeBosch BJ. Pegylated arginine deiminase drives arginine turnover and systemic autophagy to dictate energy metabolism. Cell Rep Med 2022; 3: 100498.

[64] Changou CA, Chen YR, Xing L, Yen Y, Chuang FY, Cheng RH, Bold RJ, Ann DK and Kung HJ. Arginine starvation-associated atypical cellular death involves mitochondrial dysfunction, nuclear DNA leakage, and chromatin autophagy. Proc Natl Acad Sci U S A 2014; 111: 14147-14152.

[65] Butler A, Hoffman P, Smibert P, Papalexi E and Satija R. Integrating single-cell transcriptomic data across different conditions, technologies, and species. Nat Biotechnol 2018; 36: 411-420.
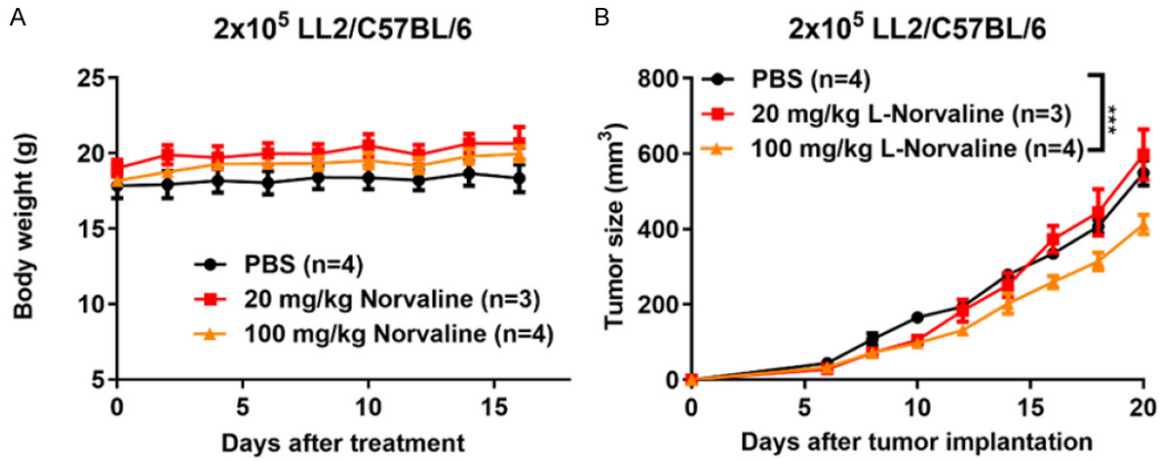
Supplementary Figure 1. 100 mg/kg L-norvaline treatment inhibits the growth of LL2 tumors. A. Body weight changes of LL2 tumor mice in 20 mg/kg and 100 mg/kg L-norvaline treatments. B. The growth curve of LL2 tumors over time for mice following different treatments. Black, red, and orange lines is PBS, 20 mg/kg L-Norvaline, and 100 mg/kg L-Norvaline treatment, respectively. The *p* value of tumor curve was calculated by two-way ANOVA. The results of the tumor growth curve are presented as the means ± SEM. *$p < 0.05$.
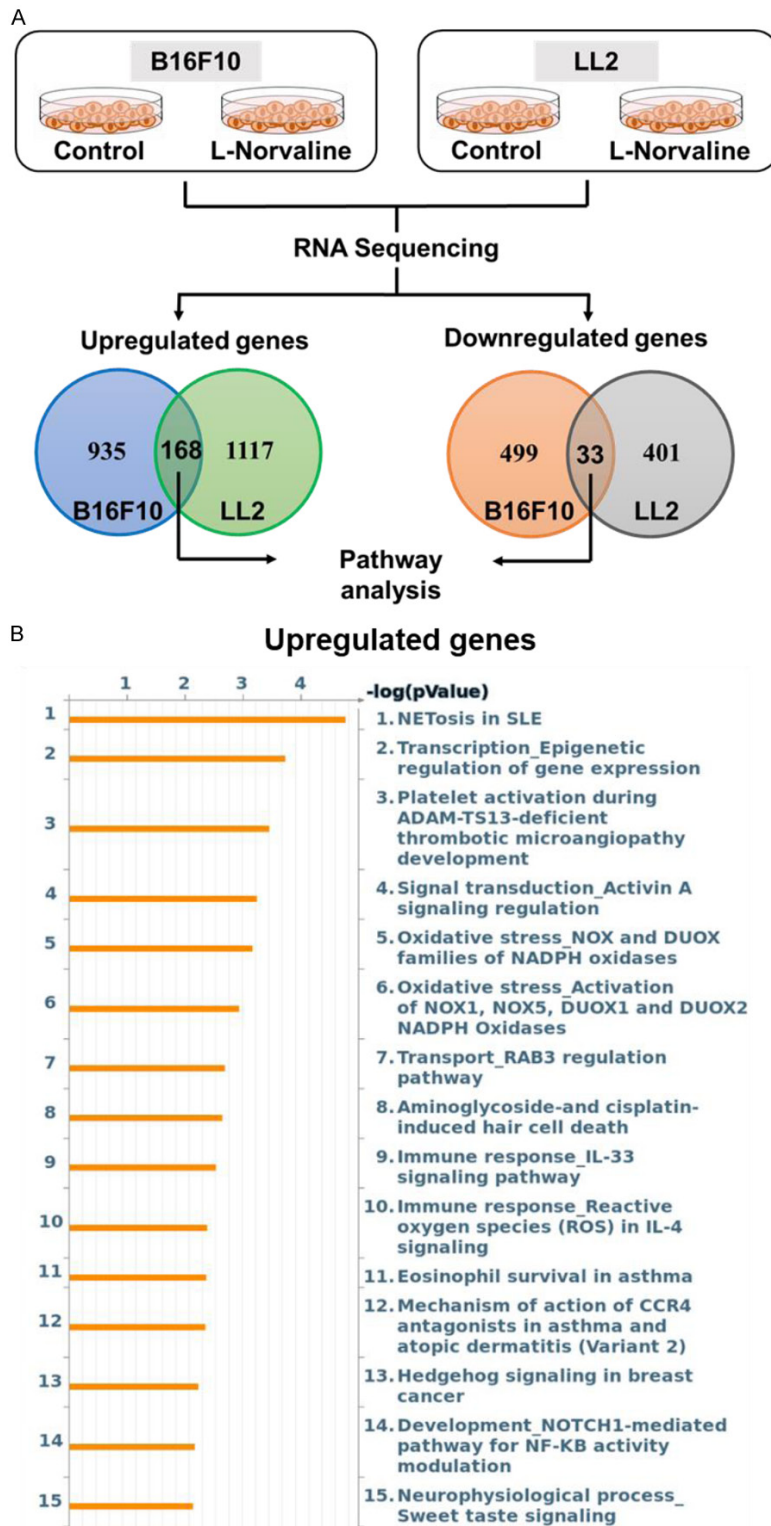
Supplementary Figure 2. L-norvaline-induced upregulated genes are involved in immune-related signaling. A. The process of genes selection. B16F10 and LL2 cancer cells were treated with or without 0.1 mg/mL L-norvaline. After three days, RNA was extracted from these cultured cells and performed on RNA sequencing. Venn diagram illustrating the distribution of differentially expressed genes and the overlap between the two L-norvaline-treated cancer cells. Upregulated genes were defined as a fold change (Nor/Ctrl) more than or equal to 1.5, and downregulated genes were defined as a fold change (Nor/Ctrl) less than or equal to 0.5. The overlapping genes (168 and 33 genes) were input to KEGG and Metacore platform for pathway enrichment analysis. B. Bar chart showing the top 15 pathways enriched for upregulated genes.

Supplementary Table 1. Overlapping upregulated genes in L-Norvaline-treated B16F10 and LL2 cells

Gene Name	Description	FC (B16F10)	FC (LL2)
Lipc	lipase, hepatic	5.48	1.67
Mst1r	macrophage stimulating 1 receptor (c-met-related tyrosine kinase)	4.98	1.93
Duxbl1	double homeobox B-like 1	4.39	1.85
Cts8	cathepsin 8	4.14	2.81
Mir8091	microRNA 8091	4.14	2.78
Unc45b	unc-45 myosin chaperone B	4.14	1.67
Podn	podocan	4.03	1.53
Bik	BCL2-interacting killer	3.89	2.78
Rab3c	RAB3C, member RAS oncogene family	3.61	1.9
Csf3	colony stimulating factor 3 (granulocyte)	3.59	1.69
Tsnaxip1	translin-associated factor X (Tsnax) interacting protein 1	3.59	4.55
Gm15328	predicted gene 15328	3.59	2.12
Pinlyp	phospholipase A2 inhibitor and LY6/PLAUR domain containing	3.53	1.85
Foxa3	forkhead box A3	3.41	1.62
Hp	haptoglobin	3.41	2.1
Mettl21c	methyltransferase like 21C	3.3	1.85
5730403I07Rik	RIKEN cDNA 5730403I07 gene	3.18	2.78
Abcb11	ATP-binding cassette, sub-family B (MDR/TAP), member 11	3.18	1.66
Epgn	epithelial mitogen	3.18	1.62
4921517D22Rik	RIKEN cDNA 4921517D22 gene	3.15	2.86
Pdzd9	PDZ domain containing 9	3.07	1.56
Bcas1	breast carcinoma amplified sequence 1	2.81	1.93
Erich5	glutamate rich 5	2.81	2.86
H60c	histocompatibility 60c	2.78	2.42
6330410L21Rik	RIKEN cDNA 6330410L21 gene	2.73	1.93
Gm16287	predicted gene 16287	2.72	1.74
0610005C13Rik	RIKEN cDNA 0610005C13 gene	2.69	2.78
1700001O22Rik	RIKEN cDNA 1700001O22 gene	2.69	2.69
Acot6	acyl-CoA thioesterase 6	2.69	1.93
Kcne2	potassium voltage-gated channel, Isk-related subfamily, gene 2	2.69	4.38
Rfx8	regulatory factor X 8	2.69	1.85
Snora2b	small nucleolar RNA, H/ACA box 2B	2.69	1.93
Spint2	serine protease inhibitor, Kunitz type 2	2.69	2.09
Srms	src-related kinase lacking C-terminal regulatory tyrosine and N-terminal myristylation sites	2.69	1.93
Dgkg	diacylglycerol kinase, gamma	2.67	1.93
Cxcl15	chemokine (C-X-C motif) ligand 15	2.57	2.68
Gm20753	predicted gene, 20753	2.57	1.93
Gpr20	G protein-coupled receptor 20	2.57	1.85
Hsh2d	hematopoietic SH2 domain containing	2.57	1.85
Nepn	nephrocan	2.57	2.86
Scnn1b	sodium channel, nonvoltage-gated 1 beta	2.57	1.85
Snora31	small nucleolar RNA, H/ACA box 31	2.54	1.52
Ano2	anoctamin 2	2.53	1.85
Snora78	small nucleolar RNA, H/ACA box 7	2.49	5.32
4930549G23Rik	RIKEN cDNA 4930549G23 gene	2.45	2.86
Ccr4	chemokine (C-C motif) receptor 4	2.45	1.93
Fam219aos	family with sequence similarity 219, member A, opposite strand	2.45	2.86
Gm3363	predicted gene 3363	2.45	3.19
Hist3h2ba	histone cluster 3, H2ba	2.45	2.69
Svopl	SV2 related protein homolog (rat)-like	2.45	1.93
Tnfsf18	tumor necrosis factor (ligand) superfamily, member 18	2.45	2.2

Vwa2	von Willebrand factor A domain containing 2	2.45	1.62
Mroh8	maestro heat-like repeat family member 8	2.44	2.12
Nkain3	Na+/K+ transporting ATPase interacting 3	2.42	2.78
Elf5	E74-like factor 5	2.42	1.93
Gm7904	predicted gene 7904	2.35	3.08
Usp17la	ubiquitin specific peptidase 17-like A	2.34	1.59
Ghrl	ghrelin	2.27	2.6
Gm3264	predicted gene 3264	2.22	2.04
Rab33a	RAB33A, member RAS oncogene family	2.17	3.79
Lhx4	LIM homeobox protein 4	2.14	1.93
Apom	apolipoprotein M	2.13	1.82
Sult6b1	sulfotransferase family, cytosolic, 6B, member 1	2.09	5.4
6030440G07Rik	RIKEN cDNA 6030440G07 gene	2.07	1.91
Hk1os	hexokinase 1, opposite strand	2.07	1.56
1810024B03Rik	RIKEN cDNA 1810024B03 gene	2.01	1.93
Gucy1a2	guanylate cyclase 1, soluble, alpha 2	2	1.79
Cacna2d2	calcium channel, voltage-dependent, alpha 2/delta subunit 2	1.94	1.85
Ceacam2	carcinoembryonic antigen-related cell adhesion molecule 2	1.92	1.85
C130060C02Rik	RIKEN cDNA C130060C02 gene	1.91	1.9
Olig3	oligodendrocyte transcription factor 3	1.9	3.59
G630055G22Rik	RIKEN cDNA G630055G22 gene	1.89	1.6
Noxo1	NADPH oxidase organizer 1	1.89	1.57
4933405L10Rik	RIKEN cDNA 4933405L10 gene	1.89	1.93
Scarna6	small Cajal body-specific RNA 6	1.89	2.1
Rprml	reprimo-like	1.87	2.06
Tmod4	tropomodulin 4	1.86	1.74
1600014C23Rik	RIKEN cDNA 1600014C23 gene	1.84	2.69
1700010B08Rik	RIKEN cDNA 1700010B08 gene	1.84	2.17
2610528A11Rik	RIKEN cDNA 2610528A11 gene	1.84	2.9
4933424G05Rik	RIKEN cDNA 4933424G05 gene	1.84	1.85
Acbd7	acyl-Coenzyme A binding domain containing 7	1.84	1.55
Ccdc180	coiled-coil domain containing 180	1.84	2.86
Chrd	chordin	1.84	2.78
Chrna10	cholinergic receptor, nicotinic, alpha polypeptide 10	1.84	1.93
Ctla4	cytotoxic T-lymphocyte-associated protein 4	1.84	3.54
Cyp26c1	cytochrome P450, family 26, subfamily c, polypeptide 1	1.84	1.85
Gcm1	glial cells missing homolog 1	1.84	1.67
Gm10390	predicted gene 10390	1.84	1.93
Gm16998	predicted gene, 16998	1.84	2.12
Gm8773	predicted gene 8773	1.84	1.71
Heatr9	HEAT repeat containing 9	1.84	1.67
Hecw1	HECT, C2 and WW domain containing E3 ubiquitin protein ligase 1	1.84	1.85
Hoxc5	homeobox C5	1.84	1.95
Il22ra1	interleukin 22 receptor, alpha 1	1.84	1.93
Mia2	melanoma inhibitory activity 2	1.84	1.93
Nccrp1	non-specific cytotoxic cell receptor protein 1 homolog (zebrafish)	1.84	1.85
Prss42	protease, serine 42	1.84	2.86
Ptprcap	protein tyrosine phosphatase, receptor type, C polypeptide-associated protein	1.84	1.67
Trpm5	transient receptor potential cation channel, subfamily M, member 5	1.84	1.68
Zcchc13	zinc finger, CCHC domain containing 13	1.84	1.93
Zscan10	zinc finger and SCAN domain containing 10	1.84	1.93
Il4i1	interleukin 4 induced 1	1.84	3.85
Dusp15	dual specificity phosphatase-like 15	1.84	1.92

Wnt11	wingless-type MMTV integration site family, member 11	1.82	1.62
Henmt1	HEN1 methyltransferase homolog 1 (Arabidopsis)	1.81	3.71
Sp7	Sp7 transcription factor 7	1.81	1.85
Dnah11	dynein, axonemal, heavy chain 11	1.8	1.93
Hhipl2	hedgehog interacting protein-like 2	1.77	2.37
Ntf5	neurotrophin 5	1.76	1.52
Hist2h2ac	histone cluster 2, H2ac	1.75	2.17
Rims1	regulating synaptic membrane exocytosis 1	1.75	3.79
Krtcap3	keratinocyte associated protein 3	1.74	1.75
4930484H19Rik	RIKEN cDNA 4930484H19 gene	1.73	2.86
4933417E11Rik	RIKEN cDNA 4933417E11 gene	1.73	1.53
5031425F14Rik	RIKEN cDNA 5031425F14 gene	1.73	2.25
8030442B05Rik	RIKEN cDNA 8030442B05 gene	1.73	1.85
Adra2b	adrenergic receptor, alpha 2b	1.73	1.85
Dusp13	dual specificity phosphatase 13	1.73	1.62
Foxn1	forkhead box N1	1.73	2.69
Frmd7	FERM domain containing 7	1.73	2.13
Gm2022	predicted pseudogene 2022	1.73	1.93
Lhfpl3	lipoma HMGIC fusion partner-like 3	1.73	2.86
Prr19	proline rich 19	1.73	2.55
Rnf224	ring finger protein 224	1.73	1.93
Slc16a5	solute carrier family 16 (monocarboxylic acid transporters), member 5	1.73	1.85
Slc4a9	solute carrier family 4, sodium bicarbonate cotransporter, member 9	1.73	1.85
Stat4	signal transducer and activator of transcription 4	1.73	1.85
Tspan1	tetraspanin 1	1.73	2.69
Cpne9	copine family member IX	1.72	1.61
Tcap	titin-cap	1.71	4.55
Gm4841	predicted gene 4841	1.68	1.56
Hist1h4c	histone cluster 1, H4c	1.68	2.05
BC030499	cDNA sequence BC030499	1.67	2.34
Gstt1	glutathione S-transferase, theta 1	1.65	3.62
Duox2	dual oxidase 2	1.65	1.85
B130006D01Rik	RIKEN cDNA B130006D01 gene	1.65	2.03
9330158H04Rik	RIKEN cDNA 9330158H04 gene	1.64	1.74
Hist1h3a	histone cluster 1, H3a	1.62	1.71
Oas1b	2'-5' oligoadenylate synthetase 1B	1.61	2.68
P2ry4	pyrimidinergic receptor P2Y, G-protein coupled, 4	1.6	1.85
Fam46c	terminal nucleotidyltransferase 5C	1.6	3.14
Snx22	sorting nexin 22	1.58	1.62
Il5ra	interleukin 5 receptor, alpha	1.58	3.54
4930590J08Rik	RIKEN cDNA 4930590J08 gene	1.57	2.06
Ndnf	neuron-derived neurotrophic factor	1.57	1.93
Aldh8a1	aldehyde dehydrogenase 8 family, member A1	1.56	1.57
Cmya5	cardiomyopathy associated 5	1.56	1.91
Gm13498	predicted gene 13498	1.56	2.11
Slc5a11	solute carrier family 5 (sodium/glucose cotransporter), member 11	1.56	1.93
Il33	interleukin 33	1.56	1.98
Atp8b5	ATPase, class I, type 8B, member 5	1.54	1.85
Sorcs2	sortilin-related VPS10 domain containing receptor 2	1.54	1.82
G630025P09Rik	RIKEN cDNA G630025P09 gene	1.54	1.74
Tmprss5	transmembrane protease, serine 5 (spinesin)	1.53	1.85
2310003N18Rik	RIKEN cDNA 2310003N18 gene	1.53	1.85
Gm12216	predicted gene 12216	1.53	1.68

|			
Rnf151	ring finger protein 151	1.53	2.98
Npc1l1	NPC1 like intracellular cholesterol transporter 1	1.52	2
4632428C04Rik	RIKEN cDNA 4632428C04 gene	1.52	1.85
Tctex1d4	Tctex1 domain containing 4	1.51	2.75
Cideb	cell death-inducing DNA fragmentation factor, alpha subunit-like effector B	1.51	2.86
Ihh	Indian hedgehog	1.5	2.98
G630064G18Rik	RIKEN cDNA G630064G18 gene	1.5	2.69
Dio2	deiodinase, iodothyronine, type II	1.5	1.87
Dhh	desert hedgehog	1.5	2.69
Hspb7	heat shock protein family, member 7 (cardiovascular)	1.5	1.9
4930447M23Rik	RIKEN cDNA 4930447M23 gene	1.5	2.86

FC abbreviation represented fold change (treatment/control).

Supplementary Table 2. Overlapping downregulated genes in L-Norvaline-treated B16F10 and LL2 cells

Gene Name	Description	FC (B16F10)	FC (LL/2)
A330041J22Rik	RIKEN cDNA A330041J22 gene	0.5	0.41
Asgr1	asialoglycoprotein receptor 1	0.48	0.24
Tnnt1	troponin T1, skeletal, slow	0.48	0.23
Hist1h2ah	histone cluster 1, H2ah	0.48	0.46
2010109I03Rik	RIKEN cDNA 2010109I03 gene	0.47	0.38
Col11a1	collagen, type XI, alpha 1	0.47	0.49
Psmb11	proteasome (prosome, macropain) subunit, beta type, 11	0.46	0.42
Gm5512	predicted gene 5512	0.45	0.01
Scube1	signal peptide, CUB domain, EGF-like 1	0.44	0.41
Lbhd1	LBH domain containing 1	0.44	0.29
Hist1h2al	histone cluster 1, H2al	0.42	0.41
Gm38415	predicted gene, 38415	0.4	0.33
Myo7b	myosin VIIB	0.4	0.41
Sox7	SRY (sex determining region Y)-box 7	0.4	0.45
Tnfrsf17	tumor necrosis factor receptor superfamily, member 17	0.4	0.35
Tub	tubby bipartite transcription factor	0.4	0.14
1810019D21Rik	RIKEN cDNA 1810019D21 gene	0.39	0.31
1700008O03Rik	RIKEN cDNA 1700008O03 gene	0.39	0.19
Acta1	actin, alpha 1, skeletal muscle	0.39	0.29
Ldlrad2	low density lipoprotein receptor A domain containing 2	0.38	0.23
Mpp3	membrane protein, palmitoylated 3 (MAGUK p55 subfamily member 3)	0.38	0.45
Skint2	selection and upkeep of intraepithelial T cells 2	0.38	0.3
Paqr5	progestin and adipoQ receptor family member V	0.32	0.19
Aurkc	aurora kinase C	0.3	0.28
Skint4	selection and upkeep of intraepithelial T cells 4	0.3	0.3
Cuzd1	CUB and zona pellucida-like domains 1	0.29	0.32
Atp1a2	ATPase, Na+/K+ transporting, alpha 2 polypeptide	0.24	0.41
Gdf5	growth differentiation factor 5	0.24	0.41
Zfp91Cntf	predicted readthrough transcript (NMD candidate), 44505	0.21	0.21
Asb5	ankyrin repeat and SOCs box-containing 5	0.15	0.28
Abca17	ATP-binding cassette, sub-family A (ABC1), member 17	0.14	0.3
Tmem254c	transmembrane protein 254c	0.14	0.01
Hnf1b	HNF1 homeobox B	0.14	0.35

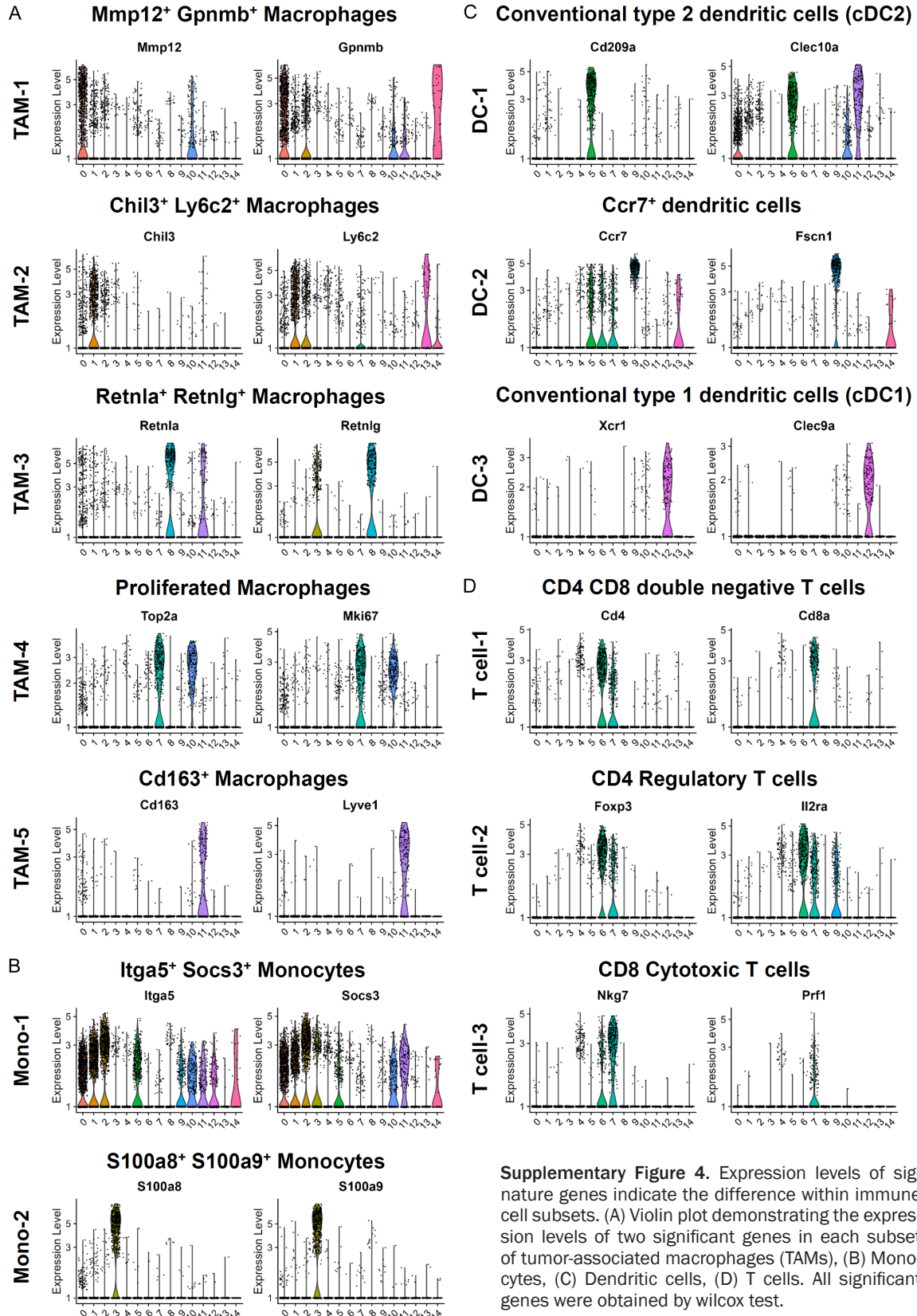FC abbreviation represented fold change (treatment/control).
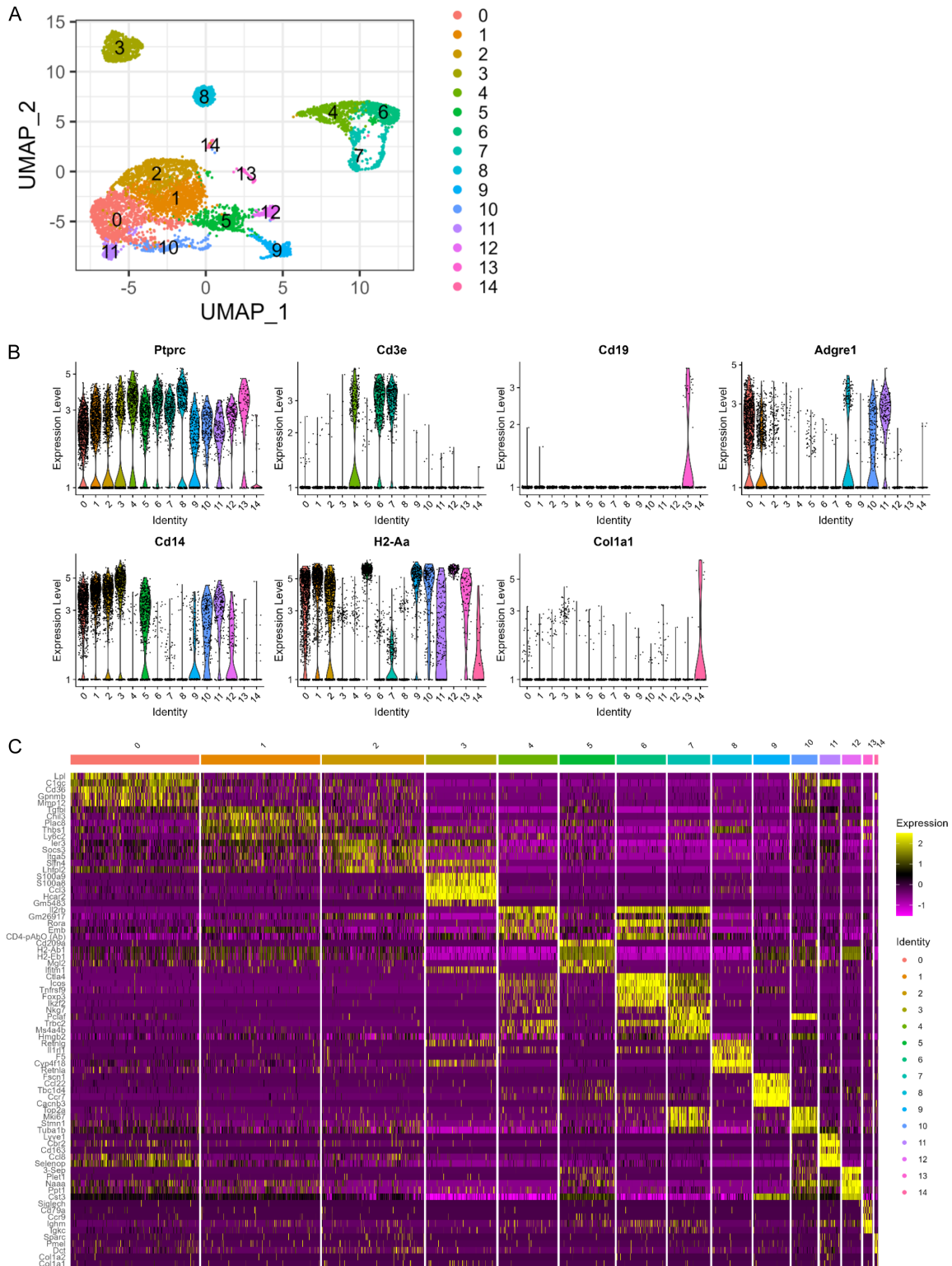
Supplementary Figure 3. Single-cell RNAseq analysis of intratumoral immune cells indicates numbers in each cell type. A. A UMAP projection analysis of infiltrated immune cells (n = 6485 cells from four 14 groups: 1085 PBS treatment, 1927 L-Norvakine treatment, 1458 ADI-PEG20 treatment, and 2015 combination treatment). B. Expression levels of common marker genes in each cluster. C. Heatmap displaying the top 5 feature genes in each clusters.
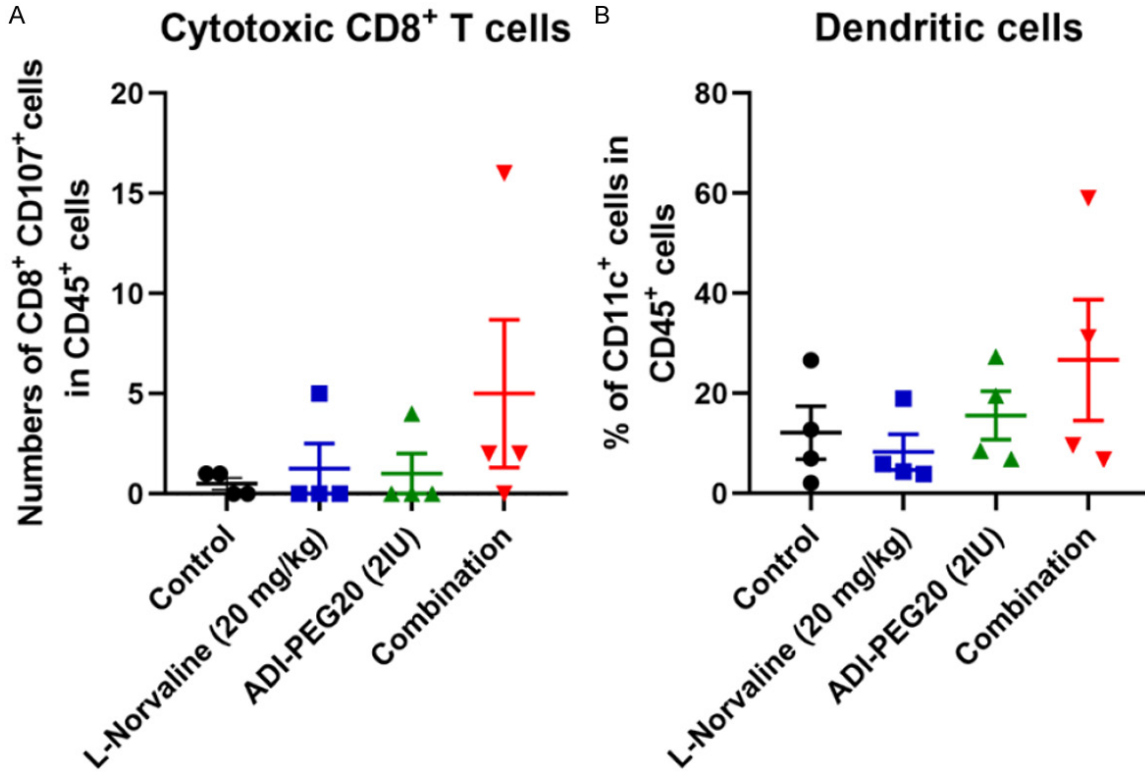
Supplementary Table 3. The characteristic in each cluster

Clusters	Cell Type	Annotation	Gene expression
0	TAM-1-Macrophages	Mmp12$^+$ Gpnmb$^+$ TAMs	Gpnmb, MMP12, Adgre1 (F4/80)
1	TAM-2-Macrophages	Chil3$^+$ Ly6c$^+$ TAMs	Ly6c, Plac8, Chil3, Adgre1 (F4/80)
2	Monocytes-1	Itg5a$^+$ Socs3$^+$ Monocytes	Itga5, Socs3, CD14
3	Monocytes-2	S100a8$^+$ S100a9$^+$ Monocytes	S100a8, S100a9, CD14,
4	T cell-1	Double negative T cells	CD3 positive, CD4 and CD8 negative
5	Dendritic cell-1	Conventional type 2 Dendritic cells	Clec10a, H2-Ab1, CD209a
6	T cell-2	CD4 Regulatory T cells	CD4, Foxp3, CD25
7	T cell-3	CD8 Cytotoxic T cells	CD8, Gzmb, Prf1, Nkg7
8	TAM-3-Macrophages	Retnla$^+$ Retnlg$^+$ TAMs	Retnlg, Retnla, Adgre1 (F4/80)
9	Dendritic cell-2	Ccr7$^+$ Dendritic cells	Fscn1, CCR7
10	TAM-4-Macrophages	Proliferated TAMs	Pclaf, Mki67, Top2a, Adgre1 (F4/80)
11	TAM-5-Macrophages	CD163$^+$ TAMs	CD163, Lyve1
12	Dendritic cell-3	Conventional type 1 Dendritic cells	Xcr1, Clec9a, Btla
13	B cells	B cells	CD79a, Ms4a1, CD19
14	Fibroblast	Fibroblast	Col6a2, Col1a1

Supplementary Figure 4. Expression levels of signature genes indicate the difference within immune cell subsets. (A) Violin plot demonstrating the expression levels of two significant genes in each subset of tumor-associated macrophages (TAMs), (B) Monocytes, (C) Dendritic cells, (D) T cells. All significant genes were obtained by wilcox test.

Supplementary Figure 5. Combination treatment of L-Norvaline and ADI-PEG20 induced an increase of infiltrated cytotoxic CD8+ T cells and dendritic cells. A. FACS analysis of the number of CD8+ CD107+ cytotoxic T cells in the TME. B. FACS analysis of the percentage of total dendritic cells in the TME. The mice were sacrificed on the 20th day after implantation of B16F10 tumor cells, and tumor infiltrating lymphocytes were analyzed. The column scatter dot plot represents the mean values ± SEMs.